Study of the role of CRMP2 during the nervous system development in zebrafish

July 2020

Carolina FIALLOS OLIVEROS

フィアヨス　オリベロス　　カロリナ

Study of the role of CRMP2 during the nervous system development in zebrafish

July 2020

Waseda University
Graduate School of Advanced Science and Engineering
Department of Life Science & Medical Bioscience
Research on Molecular Brain Science

Carolina FIALLOS OLIVEROS
フィアヨス　オリベロス　　カロリナ

CONTENTS

Abstract

Different studies have shown the importance of CRMP family proteins in several processes during nervous system development. Among others, they are involved in axonal growth and cell migration. The most studied member of this family is CRMP2, originally identified as a mediator of semaphorin signaling. However, its role *in vivo* is still being investigated.

Here I used two different technologies to analyze the function of CRMP2 in the migration of the facial motor neurons and the elongation of trigeminal axons in zebrafish. On the one hand, I used different types of antisense morpholino oligonucleotides to study the effects of CRMP2 knockdown in these processes. On the other hand, I generated a CRMP2 KO zebrafish mutant line using the CRISPR/Cas9 system to confirm these effects.

The high homology between zebrafish and human CRMP2, together with the model organism features such as the transparency of the embryos and its relatively rapid development, make it a suitable species to study this gene's functions. Furthermore, I took advantage of the Islet1-GFP line to easily analyze the development of the cranial motor neurons. This transgenic line allows the direct observation of these neurons during the early development of zebrafish.

In this study I show that CRMP2 is necessary for the proper migration of facial motor neurons during early development in zebrafish and that this gene is also required for the proper elongation of the trigeminal motor axons in this species. Both CRMP2 morphants and mutants exhibit abnormalities in the migration of the facial motor neurons from rhombomeres 4 and 5 (r4 and r5) to 6 and 7. Facial motor neurons that were expected to be at r6 by 36 hours post-fertilization (hpf) were still located at r4 and r5 at 50 hpf. Besides, after both knock-down and knock-out of CRMP2 I found deficiencies in the growth of the trigeminal axons. In morphants, axons were much shorter compared to those of wild type embryos; in mutants, axons were thin and some abnormalities in the pathfinding were also observed. The mutant phenotypes were rescued in both facial neuron migration and trigeminal axons elongation processes by injecting CRMP2 mRNA into the KO embryos.

I also analyzed the possible discrepancies between the knock-down and knock-out phenotypes. I observed the positioning of caudal primary motor neurons and the retinal axon growth in CRMP2 KO mutants. These two processes were previously studied using morpholino-induced knock-down. However, I did not observe a clear phenotype in the knock-out embryos and these differences could be due to compensation effects.

In addition, I show a possible role of CRMP2 in adult fin regeneration. CRMP2 mutants exhibit defects in the shape of their regenerated fins and, although these effects have not been studied in depth, these observations are good indicators that CRMP2 is involved in this process and, therefore, should be further studied.

Chapter 1: Introduction

1.1 Background

1.1.1 CRMP family: CRMP2

Collapsin response mediator proteins (CRMPs), also known as dihydropyrimidinase-like family (dpysls), are evolutionarily conserved cytosolic phosphoproteins expressed in several regions throughout the central and peripheral nervous systems during development (Wang and Strittmatter, 1996). They are known for being involved in axon growth, guidance and regeneration, neuronal polarity, apoptosis and cell migration in the nervous system (Schweitzer et al., 2005).

Studies in neonatal rat (Wang and Strittmatter, 1996) showed that CRMPs were expressed in the forebrain, midbrain, pons and cerebellum with different temporal and spatial regulations. They also found that CRMP2 was the most expressed since early development. CRMP2 was initially discovered as a signal-transducing molecule of the growth cone collapsing activity of semaphorins (Goshima et al., 1995) and it is thought that different CRMPs probably transduce signals from different semaphorins. In addition, CRMPs are expressed persistently in specific areas of the nervous system that undergo synaptic remodeling; this, makes it likely that semaphorin/CRMP signaling mechanisms have a role regulating synaptic plasticity in the adult nervous system (Wang and Strittmatter, 1996).

Schweitzer et al. (2005) studied the expression of the six zebrafish CRMPs (CRMP-1 to 4, 5a, 5b) between 16 and 24 hours post-fertilization (hpf) and observed a general increase in many regions undergoing axonogenesis or neuronal differentiation, but expression was not found outside the nervous system. In zebrafish, CRMP2 expression can be clearly observed at 16 hpf in different regions of the CNS such as the telencephalon or the nucleus of the tract of the post-optic commissure (NTPOC), where differentiation has already begun (Schweitzer et al., 2005). Expression is also

strong in clusters of hindbrain neurons, in the presumptive trigeminal ganglion and in the dorsally located cells in the spinal cord, corresponding to Rohon-Beard neurons growing axons at that time (Schweitzer et al., 2005). The expression of CRMP2 continues increasing during the following hours of development and by 48 hpf it is detected in more regions such as the retinal ganglion (Christie *et al.* 2006). CRMP2 expression can be observed in the brain at least until 97 hpf (Christie *et al.* 2006). Previous research in zebrafish has shown the requirement of CRMP2 for the proper positioning of neurons in the spinal cord (Tanaka *et al.* 2012; Morimura *et al.* 2013) and also for proper retinal axon growth (Liu *et al.* 2018).

- CRMP2 is required for proper positioning of Rohon-beard neurons and neural crest cells in the zebrafish spinal cord:

Tanaka et al. (2012) designed antisense morpholinos (AMOs) targeting CRMP2 and CRMP4 to study the role of these genes in the developing nervous system *in vivo*. They found that CRMP2 and CRMP4 morphants expressed abnormalities in the positioning of Rohon-beard neurons in the dorsal part of the spinal cord at 28 hpf. Rohon-beard neurons locate bilaterally in wild type embryos, but were found on the midline in both kinds of morphants. The observed phenotype was more severe in CRMP2/CRMP4 double morphants.

- CRMP2 is required for proper positioning of caudal primary motor neurons in the zebrafish spinal cord:

In 2013, Morimura et al. found that CRMP2 and CRMP4 are also required for the correct positioning of the caudal primary motor neurons in the zebrafish spinal cord. Similarly to Tanaka et al., they knocked down CRMP2 and CRMP4 using morpholinos, but this time they observed the embryos laterally at 28 hpf. They observed that, in WT embryos, the location of the cell body of the caudal primary motor neurons was restricted to the spinal cord, but the neurons of the morphants were located ectopically, outside the spinal cord.

In both studies (Tanaka et al. 2012 and Morimura et al. 2013), the phenotypes induced by the loss of function of Cdk5 and DYRK2 were also analyzed. In both cases, the phenotypes turned to be similar to those observed in CRMP2 and CRMP4 morphants. Cdk5 and DYRK2 are known to phosphorylate CRMP2 and CRMP4 and their results indicate that the phosphorylated form of these proteins is what is required for the proper positioning of Rohon-beard neurons and primary motor neurons in the spinal cord (Tanaka et al., 2012; Morimura et al., 2013).

- CRMP-2 is required for axon growth in zebrafish retinal neurons:

Another good system to study the CNS axon guidance is the visual system. Retinal axons extend ventrally from the eye to cross the midline at the optic chiasm and continue extending dorsally and posteriorly to the tectum. Zebrafish retinal axons cross the midline and project to the contralateral brain (Karlstrom et al., 1996; Liu et al., 2018).

Liu et al. (2018) found that, in zebrafish embryos, CRMP2 and CRMP4 are expressed in the retinal ganglion cell layer when retinal axons are crossing the midline. They used morpholinos to knock-down both genes and observed a reduction in the axonal growth in CRMP2 morphants and a misprojection of the axons in the CRMP4 ones.

CRMP family has an important role in the nervous system development in different species. CRMP2 is involved in several processes and it has been detected in many regions of the developing brain (Schweitzer *et al.* 2005; Christie *et al.* 2006); therefore, it might be an important piece for the proper development of the neural circuit. It is known that zebrafish CRMPs exhibit a high amino acid correlation with their human homologs (Schweitzer et al., 2005). Therefore, it is a good model to study further and understand the function of these proteins and the mechanisms involved in their regulation.

1.1.2 Zebrafish as a model organism

The zebrafish (Danio rerio) has been used for a long time as a model organism in several fields in biology (Lele and Krone, 1996). The external development and transparency of zebrafish allow us to directly observe the behavior of the cells during this process (Warga and Kimmel, 1990; Kimmel et al., 1994; Woo and Fraser, 1995). In addition, the large number of zebrafish mutants that have been created makes it a useful model for the studies of gene function (Howe et al., 2013).

- Islet1-GFP zebrafish line

The Islet1-GFP line consists of germ line-transmitting transgenic zebrafish expressing GFP (Green Fluorescent Protein) in the cranial motor neurons. Islet1 is expressed in all postmitotic motor neurons early in their development (Higashijima et al., 2000). This fluorescence can be clearly observed already at 16 hpf and at least up to day 4. This feature, together with the transparency of the embryos, enables the visualization of the cell bodies, main axons, and the peripheral branches within the muscles (Higashijima et.al, 2000). Therefore, this transgenic line can be very useful to study genes related to the motor neuron development and clarify their role in this process.

In the same study, Higashijima et al. described the development of the cranial motor neurons. They found that the facial motor neurons (VII) migrate caudally during development. At 21 hpf most of these neurons are located at the region corresponding to r4 and r5 and they start migrating caudally until they reach r6 and r7. Most of them have reached this location by 36 hpf.

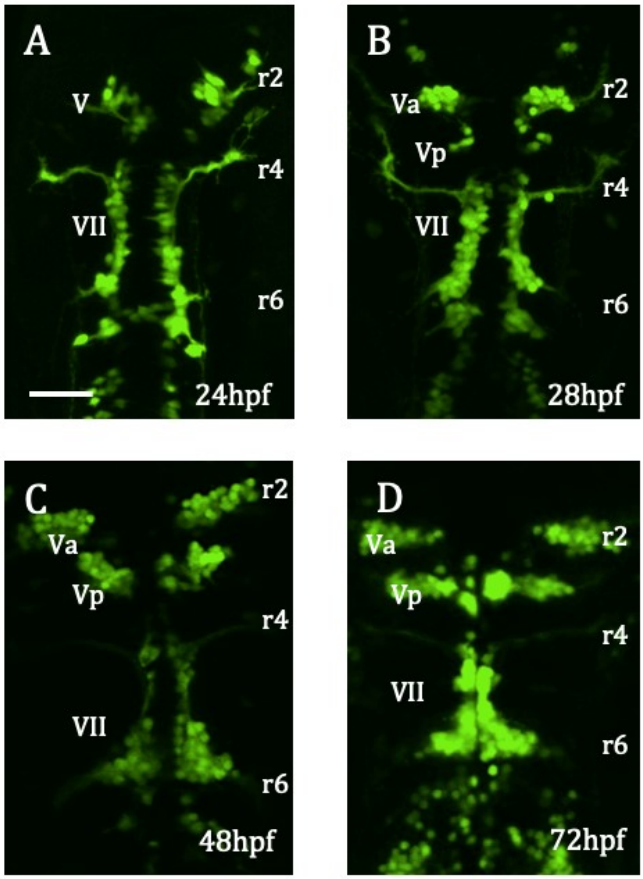

Figure 1. Dorsal view of the cranial motor neurons of Islet1-GFP zebrafish embryo from 24 to 72 hpf. A) At 24 hpf facial axons start extending and the facial neurons (VII) that were originally located in r4 and r5 migrate progressively to the caudal region. B) At 28 hpf trigeminal nucleus (V) has started to differentiate in anterior (Va) and posterior (Vp) clusters. C) At 48 hpf we can observe that most of the facial motor neurons have completed the migration process and are already located in r6 and r7 where they settle afterward (D). In all images anterior is up. Scale bar= 50 μm.

In a different study, Tanaka et al. (2007) observed the growth of the trigeminal (V) and facial (VII) motor axons using the Isl1-GFP transgenic line. They described that by 52 hpf the trigeminal motor neuron axons started to extend ventrally and at 58 hpf the growth cones of these neurons crossed the midline. Axons paused there for 4 hours and at 62 hpf the growth cones changed directions, extended posteriorly, and completed their projections by 72 hpf.

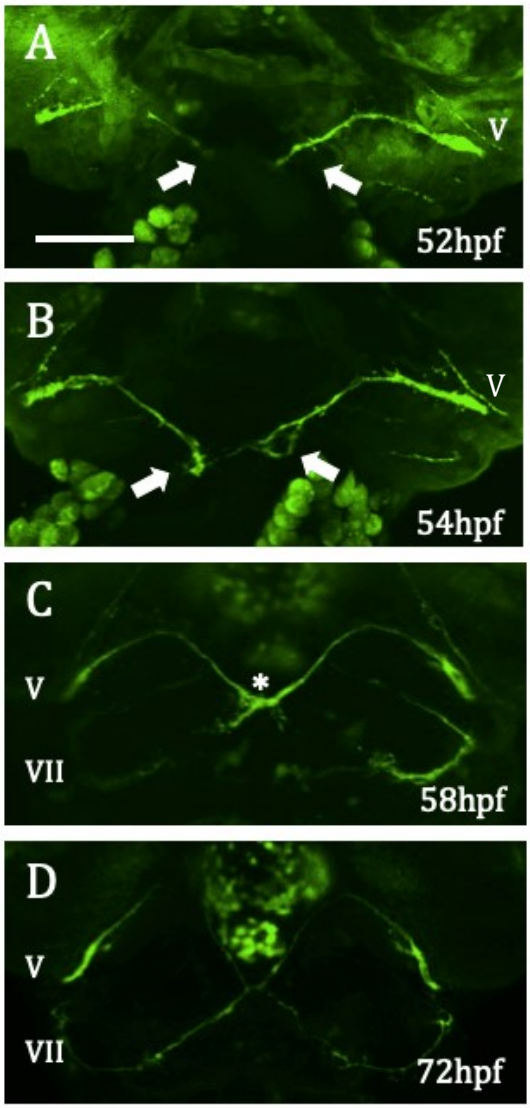

Figure 2. Ventral view of the elongation process of the trigeminal (V) and facial (VII) axons from 52 to 72 hpf in Islet1-GFP zebrafish embryo. Trigeminal axons start extending ventrally by 52 hpf and reach the boundary between first and second branchial arches by 58 hpf. They stop there for a while and restart extending posteriorly at 62 hpf until they complete their projections by 72 hpf. Arrows indicate the extending axons. The star indicates the boundary between first and second branchial arches. Anterior is up. Scale bar= 60 μm.

These findings related to both the migration of facial motor neurons and the ventral projection of facial and trigeminal axons are interesting points to study the role of genes related to neuronal migration or axon elongation such as CRMP2.

1.1.3 AMO mediated knock-down

Antisense morpholino oligonucleotides are polymers designed to block the translation of specific messenger RNAs (mRNAs) (Summerton et al., 1997) or prevent the proper splicing of the pre-mRNA (Eimon, 2014). Morpholinos bind to the complementary nucleic acid sequences by Watson-Crick base-pairing. However, a length of 25 bases is required to successfully inhibit their target mRNA and it has to be introduced in the embryo at early stages of development to be effective (Summerton et al., 1997).

Morpholinos have been found to be highly effective at low concentrations, although the effective dose has to be determined independently for each morpholino (Nasevicius and Ekker, 2000). In addition, the phenotypes induced by a morpholino-mediated knock-down can be rapidly observed in the F0. They can be classified into two types depending on the mechanism used to inhibit the target (Eimon, 2014):

1) **Translation blocking morpholinos:** this type of morpholinos binds to the mRNA start codon and blocks the progression of the ribosomal initiation complex (Eimon, 2014). These morpholinos do not degrade the target mRNA but inhibit the production of protein, both maternal and embryonic.
2) **Splicing blocking morpholinos:** this type of morpholinos block the proper processing of the target pre-mRNA, generally resulting in loss of exons or intron inclusions that will lead to non-functional protein as a product (Eimon, 2014). When using this type of morpholinos, the maternal mRNA is not inhibited.

Antisense oligonucleotides are an effective and non-expensive way to study gene function (Crooke, 1996). However, it has been shown that the phenotypes produced by knock-down techniques have a low correlation with the phenotypes of mutant zebrafish (Kok et al., 2015); thus, the benefits of using knock-down methods such as morpholino oligonucleotides has been questioned.

1.1.4 CRISPR/Cas9 system

The CRISPR/Cas9 (clustered regularly interspaced short palindromic repeats/CRISPR-associated) system is a very powerful tool to induce targeted genome modifications.
In bacteria, this system provides immunity against foreign nucleic acids (Wiedenheft et al., 2012) and it is being adapted to create a genome editing technology that is faster, cheaper and more precise than other well-known systems such as zinc-finger nucleases (ZFNs) or transcription activator-like effector nucleases (TALENs) (Hruscha et al., 2013; Gaj et al., 2013).

The CRISPR/Cas9 system requires two components to induce genome modifications: a small guide RNA (gRNA or sgRNA) and the Cas9 endonuclease. The gRNA contains the complementary sequence to the target site and the Cas9 recognizes a protospacer adjacent motif (PAM site) next to the target sequence. After binding, the Cas9 endonuclease interacts with the gRNA, inducing the cleavage of the double-strand. Typically, the non-homologous end-joining (NHEJ) repair pathway activates after the double stand break. This frequently generates insertions or deletions that can lead to frameshift mutations and therefore to premature stop codons. In case a DNA template is given, the homology-directed repair (HDR) activates instead, this pathway is convenient to induce knock-ins or concrete genome modifications (Gong et al., 2005; Reis, 2014).

Due to the simplicity of its mechanism, the CRISPR/Cas9 system can be used to induce multiple mutations simultaneously (Cong et al., 2013).

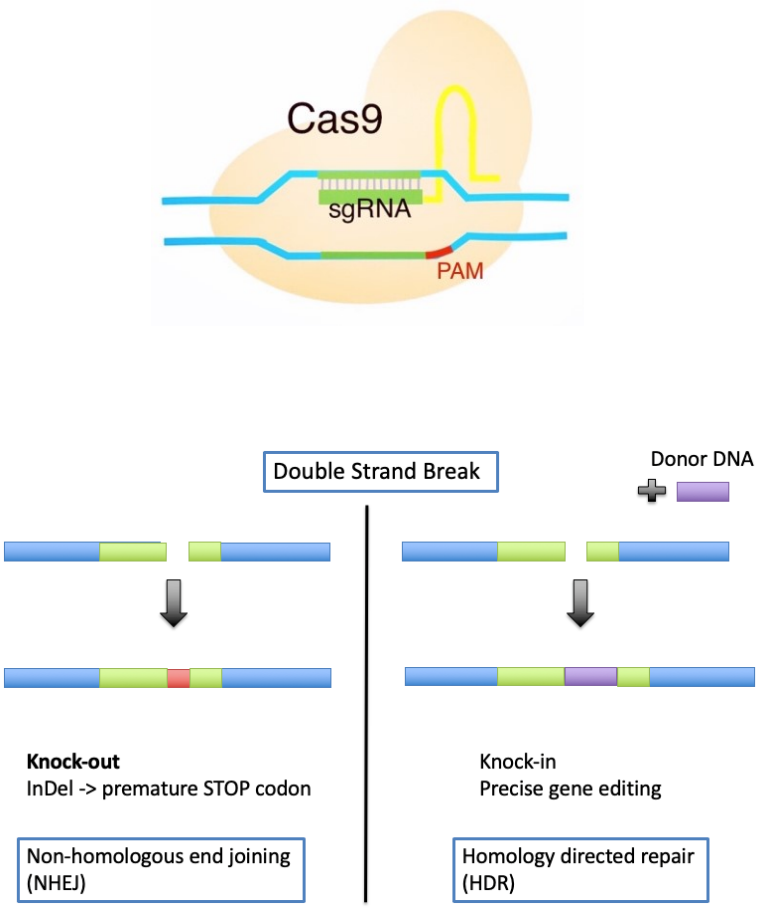

Figure 3. Scheme of the CRISPR/Cas9 induced double-strand break and the repair pathways that activate accordingly. Cas9 recognizes the PAM site and interacts with the gRNA, whose sequence is complementary to the target site. This interaction produces a double-strand cleavage. As a consequence, the NHEJ repair pathway activates, usually inducing insertions or deletions. In the presence of donor DNA, the HDR pathway allows the induction of precise mutations and knock-ins.

1.1.5 Knock-down versus knock-out methods

There is evidence of the low correlation between phenotypes induced by a knock-down and the ones that result from a knock-out. Several genes have been studied using both morpholinos and genome editing techniques and in many cases the phenotypes found after knocking down these genes were absent in the mutant embryos (Kok et al., 2015).

The discrepancies between knock-down and knock-out studies might be explained by different reasons: some researchers point out that morpholino experiments often generate off-target effects and doubt about their reliability (Kok et al., 2015); others consider that the knock-out of a gene can have consequences such as transcriptional adaptation and, as a result, mutants would show a different phenotype (Rossi et al., 2015). The fact is that both systems have advantages and disadvantages. Knock-out techniques have the precision and efficiency and let us generate mutant lines for the study of several genes; however, a gene knock-down can be very useful in situations when the knock-out is lethal or when compensatory responses to the gene deletion are observed (Zimmer et al., 2019). In conclusion, both knock-down and knock-out studies are useful and can complement each other.

1.2 Purpose of this research

New technologies are rapidly evolving, giving us more options for the study of the genes and mechanisms involved in different processes during development.
Previous studies have demonstrated the importance of CRMPs in the development of the nervous system, although their roles *in vivo* are still being studied. CRMPs are important pieces during this process and understanding better their roles and regulation could help to elucidate the reasons why some diseases are developed. Therefore, by studying the process and its components, ways to cure or prevent different disorders can be found.

Here I used zebrafish for its high homology with humans and for all the advantages mentioned before, such as its easy manipulation, to investigate deeper a member of the CRMP protein-family: CRMP2.
I took advantage not only of the quickness of the AMO knock-down but also of the efficiency of a more recent technology, the CRISPR/Cas9 system. These tools help us to study how much CRMP2 is implicated in the development of the nervous system.

Since the role of CRMP2 in axonal growth and cell migration is well known, I expected to observe clear defects in the migration of the facial motor neurons from r4 and r5 to r6 and r7. I also foresaw abnormalities in the trigeminal and facial axons elongation. To prove these hypotheses, I used the Islet1-GFP zebrafish line, which allows a more direct observation.

Thus, the main objectives of this study were:

1. Study the role of CRMP2 in the migration of facial motor neurons.
2. Study the role of CRMP2 in the elongation of trigeminal axons.
3. Establish a CRMP2 KO zebrafish mutant line.
4. Compare the mutant phenotypes with the AMO induced ones.

My hypothesis was that deficiencies would be observed in the migration of the cranial motor neurons and the elongation of the trigeminal and facial axons. I also hypothesized that, if CRMP2 has a role in these processes, abnormalities would be observed in both AMO and CRISPR/Cas9 induced morphants and mutants.

Chapter 2: Materials and methods

2.1 Animals

Zebrafish (Danio rerio) were maintained according to standard procedures (Westerfield, 2000). Zebrafish embryos were incubated at 28.5 ºC as indicated by Kimmel *et al.* (1995). To prevent pigmentation, 0.003% 1-phenyl-2-thiourea (PTU; Nacalai Tesque, Kyoto, Japan) was added to the fish water before 24 hpf (Westerfield, 2000). RIKEN Wako (RW) wild type and Islet1-GFP (*Tg(isl1:GFP)rw0*) transgenic zebrafish strains were obtained from the Zebrafish National BioResource Center of Japan (https://shigen.nig.ac.jp/zebra/). Adult zebrafish are defined as those that are 3 months or older. All experiments were performed in accordance with protocols approved by the Institutional Animal Care and Use Committee at Waseda University (2017-A029, 2018-A005 and 2019-A027).

2.2 Generation of a CRMP2 KO mutant line

2.2.1 Design

To generate a CRMP2 KO by using the CRISPR/Cas9 system, sgRNA and Cas9 mRNA were synthesized using the mMessage mMachine Kit (Ambion, Austin, Texas).
To produce the sgRNA, I selected 5'- GGAGAAAATCTAATAGTGCC - 3' as the target sequence and selected the sequences of the oligonucleotides, partial sequences of sgRNA, as follows. Oligo 1: 5' – TAGGAGAAAATCTAATAGTGCC - 3'; Oligo2: 5'- AAACGGCACTATTAGATTTTCT -3' (eurofins, Tokyo, Japan) (Fiallos-Oliveros and Ohshima, 2020).
The oligo sequences were combined and integrated into a DR247 plasmid, which was a gift from Keith Joung (Addgene plasmid #42250; http://n2t.net/addgene:42250; RRID:Addgene_42250) (Hwang *et al.* 2013). pT3TS-nCas9n was a gift from Wenbiao Chen (Addgene plasmid #46757; http://n2t.net/addgene:46757; RRID:Addgene_46757) (Jao *et al.* 2013). E. coli DH5α Competent Cells were transformed and cultured overnight at 37ºC and, after plasmid DNA extraction, the inclusion of the sequence was confirmed by sequencing. Plasmids containing the CRMP2 sequence and Cas9 sequence were digested with DraI and XbaI respectively and purified prior to mRNA synthesis.

2.2.2 CRISPR/Cas9 and mRNA injections

Previously synthesized CRMP2 sgRNA and Cas9 mRNA were co-injected into 1 to 2 cell stage zebrafish embryos. Each embryo was injected with about 0.5 nl of a solution containing a mixture of about 300 ng/µl sgRNA, 900 ng/µl Cas9 mRNA, 250 ng/µl GFP mRNA, and 0.05% Phenol Red (PR) (Fiallos-Oliveros and Ohshima, 2020). GFP mRNA was used as an indicator to confirm the success of the injection.

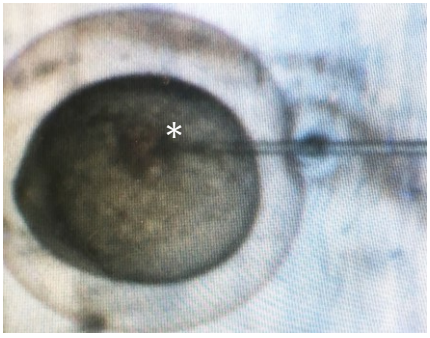

Figure 4. Microinjection procedure in a one-cell stage embryo. Phenol Red facilitates the visualization of the injected solution. The injection point is indicated with a star.

For rescue experiments, mRNA was synthesized using the mMessage mMachine Kit (Invitrogen by Thermo Fisher Scientific, Vilnius, Lithuania). Then, this mRNA was co-injected with mCherry mRNA into 1 to 2 cell stage mutant embryos.

2.2.3 Identifying the mutation

As described in Fiallos-Oliveros and Ohshima (2020), genomic DNA (gDNA) was extracted from CRISPR/cas9 injected embryos as a first screening to confirm the success of the knock-out generation. The target region was amplified by PCR using the following primers: CRMP2 forward, 5'- CCTCTAAACGTGGCCCCTGA -3'; CRMP2 reverse, 5'- ATACCACCAGGCATCACCAT -3'. PCR products were cloned into a plasmid using the pGEM T-easy vector (Promega, Madison, Wisconsin). E. coli DH5α Competent Cells were used for the consequent transformation. Cells containing the plasmid were cultured overnight in plates containing ampicillin and X-gal. Plasmid DNA was extracted from single white-colonies incubated overnight in LB media containing ampicillin. The isolated DNA was sequenced by Fasmac (Atsugi, Japan). Sequences were compared to the WT ones to identify possibly induced mutations.

After 2 months, gDNA was extracted from grown fish to identify a mutation carrier to establish a mutant line. A male fish identified as containing different mutant sequences was crossed with a WT female and some fish in the offspring were analyzed the same way as described before. After a specific mutation was identified in the descendants, primers to identify other fish carrying the same sequence were

designed as follows. CRMP2 forward, 5'- TCGCGATGCCGGCTCAGAAT -3'; CRMP2 WT reverse, 5'- GGTTTTCACCCCACCGGGCA -3'; CRMP2 Mutant reverse, 5`- GTTTTCACCCCACCGGGTGA -3' (Fasmac, Atsugi, Japan).

gDNA from the following generations was extracted either from the caudal fin of an adult fish or from the posterior half of an embryo's body.
F1 fish were crossed with Islet1-GFP, a transgenic line expressing GFP in the cranial motor neurons, allowing their direct visualization (Higashijima et al. 2000).

2.3 AMO injections

The sequences for the morpholinos (Gene Tools, Philomath, Oregon) blocking the translation of CRMP2 (*dpysl2*) and for the control morpholino were used as described previously (Tanaka et al., 2012; Morimura et al., 2013). The sequence for the splicing blocking AMO of CRMP2 was 5'-CACTCTGGAAACACAGATAAACACA- 3'. Approximately 0.5 nL of AMO (0.5 nM) was injected into 1 to 2 cell stage embryos as described (Nasevicius and Ekker, 2000).

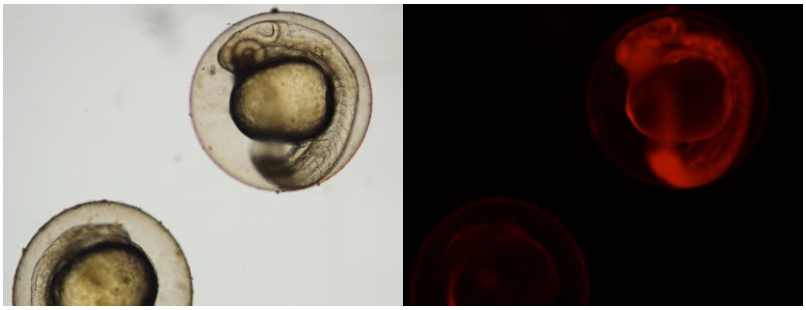

Figure 5. Bright-field (left) and fluorescence microscopy (right) images of 50 hpf embryos injected with CRMP2 AMO and mCherry mRNA. Successfully injected embryos express red fluorescence in their bodies.

2.4 DiI injection

Labeling of the retinal axons was performed using 1,1'-dioctadecyl-3,3,3'3'-tetramethylindocarbocyanine perchlorate (DiI; Invitrogen by Thermo Fisher Scientific, Eugene, Oregon). Before labeling, embryos were fixed at 4 dpf in 4% paraformaldehyde (PFA). Fixed embryos were embedded in 1.5% low melting point agarose and injected directly in the retina with DiI solution (2 mg/ml in ethanol) using a microinjector (Eppendorf AG FemtoJet 5247, Hamburg, Germany). Injected embryos were incubated overnight at room temperature and labeled axons were observed by laser-scanning confocal microscopy.

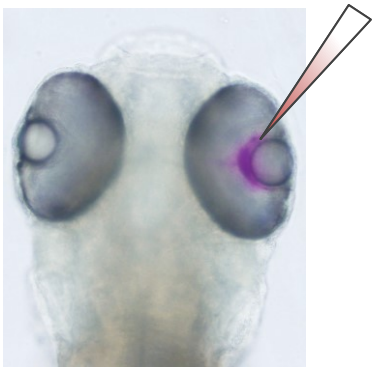

Figure 6. Representation of the DiI injection in the retinal axons. The needle is depicted in red and white. In purple, the region injected with DiI dye. Anterior is up.

2.5 Immunohistochemistry

Immunohistochemistry was performed as previously described (Tanaka et al., 2007). Embryos were fixed at 28 hpf in 4% PFA. Monoclonal anti-tubulin, acetylated antibody produced in mouse (1:2000; Sigma- Aldrich, St. Louis, Missouri) was used as a primary antibody and it was visualized using Histofine Simple Stain MAXPO (M; Nichirei, Tokyo, Japan) under conventional microscopy. Incubation with primary antibody and staining with Histofine were performed at 4ºC overnight. Prior visualization, samples were developed using 3,3′-Diaminobenzidine (DAB) at room temperature during a maximum of 1 hour.

2.6 Microscopy and imaging

For conventional microscopy a BX50 microscope (Olympus) with a UPlanApo 20x (NA= 0.70) objective was used. For fluorescence microscopy, a confocal laser scanning microscope (FV1000, Olympus) with UNPlanFL 20x (NA= 0.50) and LUMPlanFLN 40x (NA= 0.80) water immersion objectives was used. The images were captured as Z-stacks; serial optical sections were taken at intervals of 0.5 μm. The number of sections differed according to the observed region and the position of the embryo; around 15 planes were taken to observe the facial motor neurons, while more than 20 planes were necessary to ensure the complete visualization of the trigeminal axons. The images were processed using Adobe Photoshop and Adobe Illustrator.

2.7 Data analysis

As described in Fiallos-Oliveros and Ohshima (2020), I used ImageJ to measure the area of facial motor neurons occupying the regions from r4 to r5 and from r5 to r6. The sample was considered WT-like when the r5-r6 area was considerably bigger than r4-r5 (2.5 times or more); slightly affected when the region from r5 to r6 was between 1.5 and 2.4 times bigger than r4 to r5 and; severely affected if r5-r6 had a similar or smaller size than r4-r5 (less than 1.4 times bigger).

IBM SPSS Statistics 25 was used for statistical analysis. A chi-squared test was performed to determine whether the differences in frequencies between groups were statistically significant. When comparing two groups, a P-value< 0.05 indicated significant differences. When comparing three or more groups, a post hoc was performed after the chi-squared test (Beasley and Schumacker, 1995); the z scores were analyzed to determine a new specific P-value and determine which group was significantly different from the others. The new P-values are indicated in the corresponding figures.

Chapter 3: Results

Chapter 3: Results

3.1 CRMP2 knock-down (AMO injection)

Different types of AMOs targeting CRMP2 were injected into 1 to 2 cell stage embryos obtained by crossing WT and Islet-1 GFP line zebrafish.

I used either a translation blocking or a splicing blocking AMO to knock-down CRMP2 and a control AMO to confirm that the effects were due to the knock-down, not to the AMO injection. Solutions containing different concentrations of splicing blocking morpholino were injected to test the most appropriate one. After injection of 0.5 nl of splicing blocking AMO at concentrations between 0.3~0.6 mM, most samples exhibited similar phenotypes. However, when using low concentrations of about 0.25 mM the rate of samples exhibiting abnormalities decreased considerably, and when using a concentration higher than 0.6 mM the mortality rate of the embryos during the first 24 hours increased. For this reason, 0.5 mM was selected as a proper concentration for this study. After this step, the three different types of AMOs were injected always at the same concentration.

3.1.1 CRMP2 knock-down affects the migration of the facial motor neurons

AMO injected and uninjected samples were fixed at 50 hpf, time at which most of the facial motor neurons are expected to be at r6. Embryos were observed dorsally to confirm whether the migration from r4 and r5 to r6 and r7 was completed. Results showed clear abnormalities in 83.9% of the translation blocking injected embryos (n= 31) and 83.7% of the splicing blocking AMO injected ones (n= 43) (9.3% slightly and 74.4% severely affected). In these embryos, neurons failed to migrate caudally and remained distributed along the facial nucleus [Fig. 7 (C, D)]. Embryos injected with translation blocking AMO exhibited a more severe phenotype in which the trigeminal nucleus was also affected. In both uninjected or control AMO injected embryos the migration of the facial motor neurons was not affected in most cases

[Fig. 7 (A, B)]. On the other hand, only 15% of the uninjected embryos (n= 33) and 22.5% of the control AMO injected samples expressed some kind of abnormalities (n= 40). These observations suggest a role of CRMP2 in the migration of the facial motor neurons during development (Fiallos-Oliveros and Ohshima, 2020).

3.1.2 CRMP2 knock-down affects the growth of the trigeminal axons

As a next step, some splicing blocking AMO injected and uninjected samples were fixed after 58 hpf to analyze whether the axons of the trigeminal motor neurons had extended properly in the ventral direction and had crossed the midline as expected. In this case 80.0% of the samples (n= 15) showed clear defects in the axonal growth. In these embryos, the trigeminal axons were far to encounter each other in the midline, as if they just started extending ventrally [Fig. 8 (B)].

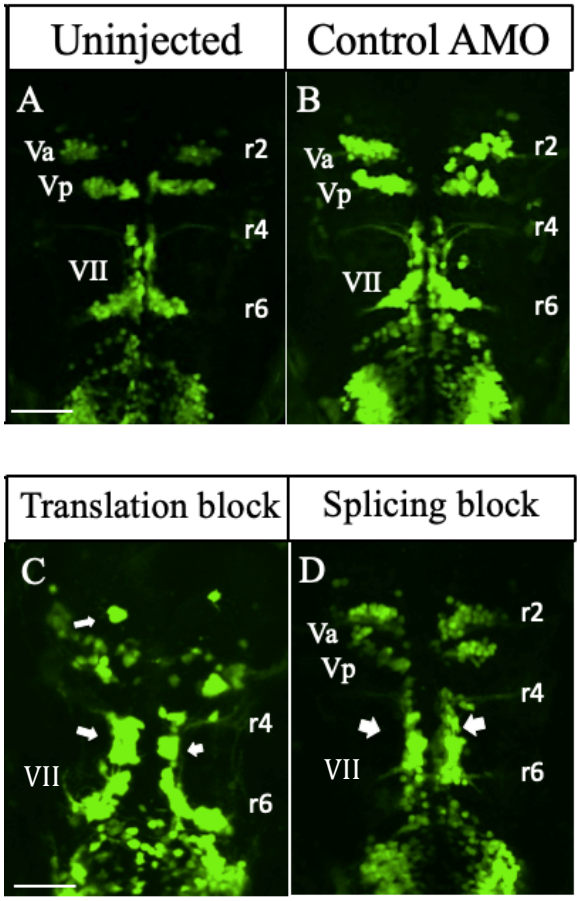
Uninjected
Control AMO
A
B
Va
Vp
VII
r2
r4
r6
Translation block
Splicing block
C
D

E

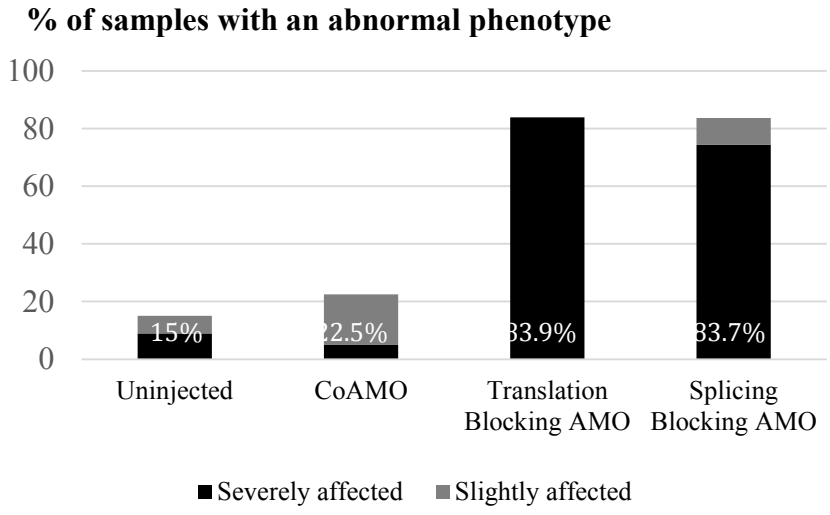
% of samples with an abnormal phenotype
100
80
60
40
20
0
15%
22.5%
83.9%
83.7%
Uninjected
CoAMO
Translation Blocking AMO
Splicing Blocking AMO
Severely affected
Slightly affected

Figure 7. Representative images of the dorsal view of the cranial motor neurons of uninjected (A), control AMO injected (B), translation blocking AMO injected (C), and splicing blocking AMO injected (D) embryos at 50 hpf. Abnormalities in the distribution of both trigeminal (Va, Vp) and facial (VII) motor neurons are clearly observed in the morphants. Abnormalities are indicated with arrows. Anterior is up. Scale bar= 50 μm. E) Percentage of embryos with an abnormal phenotype (slightly or severe) in the facial motor neurons migration at 50 hpf in uninjected (n= 33), control AMO injected (n= 40), translation blocking AMO injected (n= 31) and splicing blocking AMO injected (n= 43) (Fiallos-Oliveros and Ohshima, 2020).

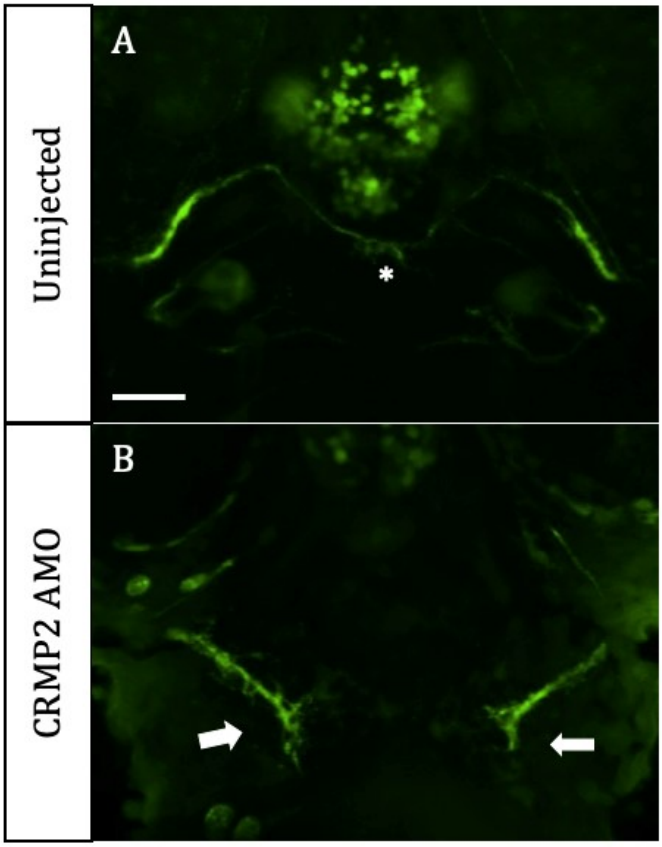

Figure 8. Ventral view of the cranial region at 58 hpf. In the uninjected embryo (A) trigeminal axons have extended ventrally and cross the midline (indicated with a star). The splicing blocking AMO injected embryo (B) exhibits shorter axons, far to reach the midline and encounter each other. Abnormalities are indicated with arrows. Anterior is up. Scale bar= 50 μm.

3.2 CRMP2 knock-out (CRISPR/Cas9)

3.2.1 Generating mutations with CRISPR/Cas9

Approximately 144 embryos were injected with about 0.5 nl of a solution containing a mixture of about 300 ng/µl sgRNA, 900 ng/µl Cas9 mRNA, 250 ng/µl GFP mRNA and 0.05% Phenol Red (PR). GFP mRNA was used as an indicator to confirm the success of the injection. One day after the injection, more than 1/3 of the embryos were dead. 34 of the embryos that survived exhibited GFP fluorescence, meaning that they were successfully injected. Then, genomic DNA from 10 of these embryos was extracted to confirm the success of the procedure. WT embryos were used as control. In total, I selected 10 GFP^+ embryos and 10 WT embryos; however, only two embryos of each group were genotyped individually, the remaining 8 embryos in each group were mixed as one sample. A fragment of CRMP2 sequence containing the target site was amplified by PCR. Interestingly, the amplicons corresponding to the injected embryos exhibited slightly different bands compared to the WT ones [Fig. 9 (A)].

Two months later, when the fish grew sufficiently, I selected three CRISPR/Cas9 injected fish and cut their caudal fins for gDNA extraction and posterior sequencing. As a control I used a WT fish. Once I amplified the fragment of interest from the DNA of these fish, I found out that the PCR band corresponding to one of the injected fish was different from the others [Fig. 9 (B)]. Later, sequencing results of different samples belonging to the same injected fish showed that diverse mutations had occurred at the target site [Fig. 9 (D)]. A mosaic mutant was identified.

A)

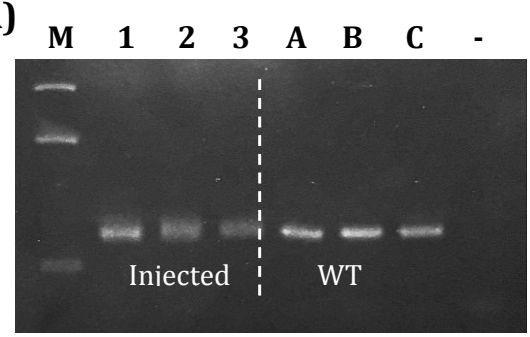

B)

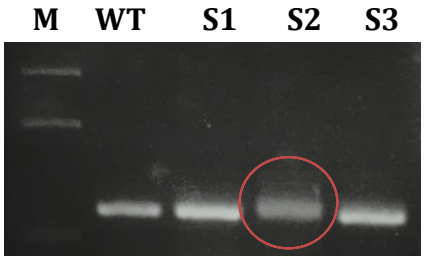

C) CRMP2 WT sequence:

…CAAATTGGAGAAAATCTAATAGTGCCCGGTGGGGTGAAAACC

Q I G E N L I V P G G V K T

ATCGATGCCCATGGGCGCATGGTGATGCCTGGTGGTATGATG…

I D A H G R M V M P G G I D …

D) CRMP2 mutant sequences (S2):

1. …CAAATTGGAGAAAATCTAATAGTTGCCCGGTGGGGTGAAAAC

Q I G E N L I V A R W G E N

CATCGATGCCCATGGGCGCATGGTGATGCCTGGTGGTATTGATGT…

H R C P W A H G D A W W Y *

2. …CAAATTGGAGAAAATCTAATAGTTTCCCCCCGGTGGGGTGAAAAC

Q I G E N L I V S P R W G E N

CATCGATGCCCATGGGCGCATGGTGATGCCTGGTGGTATTGATGT…

H R C P W A H G D A W W Y *

Target site / Disrupted target site
Coding sequence
Insertion PAM site
aa sequence * STOP codon

Figure 9. A) Amplicons corresponding to individual CRISPR/Cas9 injected embryos (1, 2) and a mixture of 8 injected embryos (3); and amplicons corresponding to individual WT embryos (A, B) and a mixture of 8 WT embryos (C). The bands corresponding to the injected embryos are slightly different compared to the WT. B) CRMP2 PCR products from uninjected WT and CRISPR/Cas9 injected grown fish. S2 exhibits a slightly different band. C, D) Fragment of CRMP2 WT sequence and fragments of CRMP2 mutant sequences found in one of the CRISPR/Cas9 injected fish (S2). Different mutations were found in the sequences corresponding to the same fish that resulted in a different PCR band after genotyping. These mutations are located at the target site and lead to a premature stop codon.

3.2.2 Identification of the mutants

When the male fish previously identified as carrying mutations in the CRMP2 sequence was ready for mating, I crossed it with a WT female. Initially, I got 301 embryos from this mating; 240 of them survived the first 24 hours, but after 2 weeks only 32 were still alive. In the next mating I got 187 embryos; 163 of them survived the first day, but a few weeks later there were only 12 left. When the surviving F1 fish became big enough, some of them were genotyped by sequencing. Sequences from 4 different fish were read and the same mutation was identified in 3 of these heterozygous fish [Fig. 10(A)]. In the F1 only two types of sequences were found: a WT sequence or a specific mutant sequence consisting in one nucleotide insertion in the target site, 3bp upstream to the PAM site; this insertion led to a premature stop codon, disrupting the gene of interest. Due to the mutation, the original CRMP2 amino acid sequence of 573 aa was shortened to 71 aa (Fiallos-Oliveros and Ohshima, 2020). I designed primers containing this specific mutant sequence and the corresponding WT one (see materials and methods) to easily identify fish carrying this mutation. These primers turned out to be very effective to determine if the gDNA of the following generations corresponded to a WT, mutant homozygote or heterozygote fish.

3.2.3 Establishing a mutant line

Once a specific mutation was identified, the F1 fish carrying it were crossed with Islet1-GFP line zebrafish to enable the direct observation of the cranial motor neurons in the CRMP2 mutants.

It was intended to establish a CRMP2 KO line by mating the fish carrying the same mutation and consecutively mating the homozygous offspring. However, the death rate of the descendants of the homozygous fish was so high that it was difficult to grow them or even analyze their phenotype. For this reason, the study of CRMP2 KO phenotype was performed using heterozygous parents or heterozygous x homozygous crosses in most of the cases. There were a few cases in which homozygous x homozygous matings worked. Due to the difficulties to establish a

homozygous line, only the anterior half of the embryos was used for phenotype observation, the posterior half was used for genotyping.

A) CRMP2 WT sequence

…CAAATTGGAGAAAATCTAATAGTGCCCGGTGGGGTGAAAACC

Q I G E N L I V P G G V K T

ATCGATGCCCATGGGCGCATGGTGATGCCTGGTGGTATGATG…

I D A H G R M V M P G G I D …

B) CRMP2 mutant sequence:

…CAAATTGGAGAAAATCTAATAGTCACCCGGTGGGGTGAAAAC

Q I G E N L I V T R W G E N

CATCGATGCCCATGGGCGCATGGTGATGCCTGGTGGTATTGATGT…

H R C P W A H G D A W W Y *

Target site / Disrupted target site
Insertion PAM site
aa sequence * STOP codon

C)

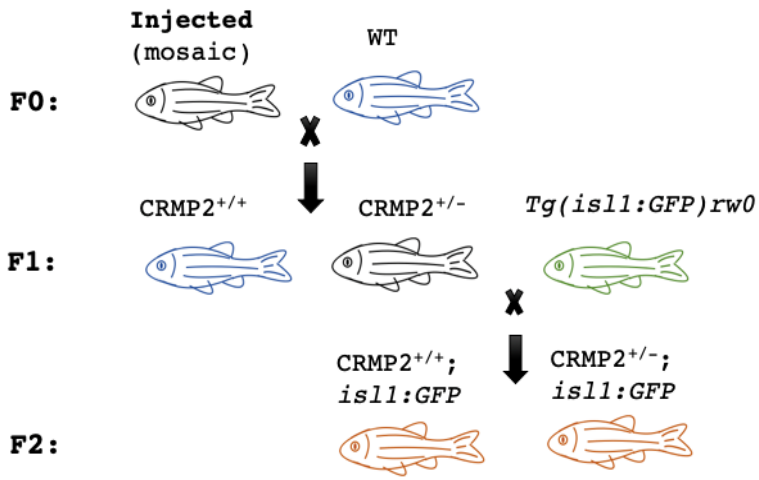

Figure 10. A, B) Comparison between WT and mutant fragments of CRMP2 sequence in which the target site is located. A 1bp insertion (G->CA) occurred 3bp upstream to the PAM site leading to a frameshift mutation and its consequent premature stop codon. Dashed lines indicate the sequence corresponding to the new primers synthesized.
C) Scheme of the crosses performed to obtain the CRMP2 KO line. The mosaic fish carrying mutations induced by CRISPR/Cas9 injection was crossed with a WT fish. Subsequently, the heterozygous descendants carrying the same specific mutation were crossed with Islet1-GFP to facilitate the observation of the cranial motor neurons in the following generations (Fiallos-Oliveros and Ohshima, 2020).

3.2.4 Immunohistochemistry

Once I generated a CRMP2 KO mutant line, I proceeded to the study of its phenotypes. First of all, I decided to confirm whether the abnormalities observed by Morimura et al. (2013) in the positioning of caudal primary motor neurons were also present in the mutants. Embryos were fixed at 28 hpf and, after tubulin immunostaining, observed laterally.

I compared WT and mutant samples; however, I did not observe ectopically located neurons in any of them (7 CRMP2$^{-/-}$, 3 CRMP2$^{+/-}$ and 10 WT embryos). Due to the quality of the staining it was difficult to detect other milder deficiencies that could have occurred, but the cell bodies of the caudal primary motor neurons were located in the spinal cord irrespective of the genotype (Fig.11). These results pointed out a discrepancy with the previously published studies.

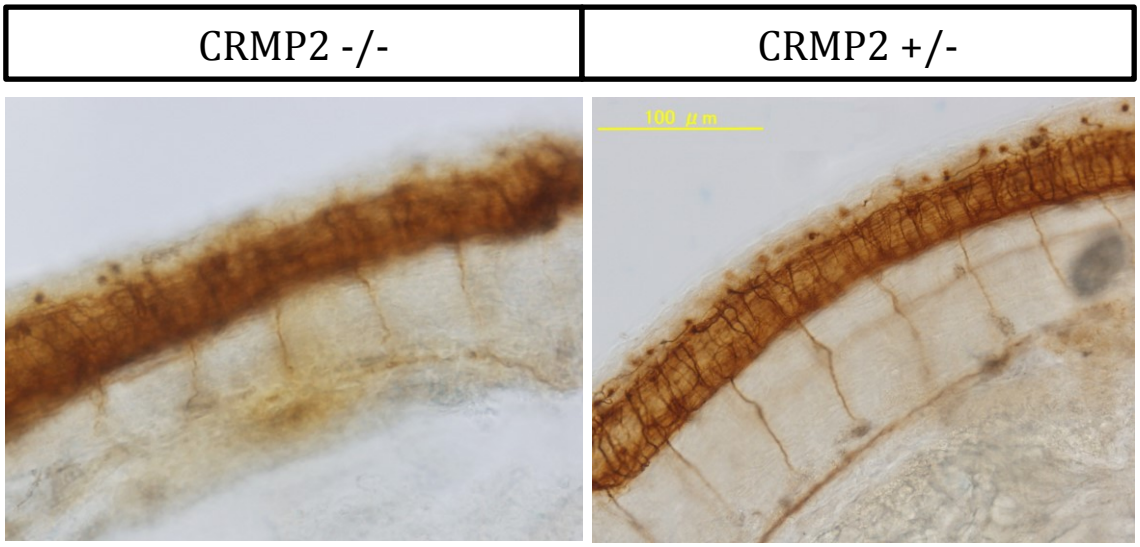

Figure 11. Lateral view of CRMP2 mutant embryos at 28 hpf. Homozygous on the left; heterozygous on the right. In both cases cell bodies are confined in the spinal cord. Dorsal is up.

3.2.5 CRMP2 knock-out affects the migration of facial motor neurons

CRMP2 KO embryos expressing GFP in the cranial motor neurons were fixed at 50 hpf for dorsal observation. Similarly to the CRMP2 AMO-injected samples, defects were observed in the migration of the facial motor neurons from r4 and r5 to r6 and r7. 77.4% of the observed samples (n= 31) exhibited some degree of abnormalities (Fiallos-Oliveros and Ohshima, 2020).

Even though most samples expressed abnormalities in the facial nucleus, not all samples expressed the same deficiency patterns or abnormalities at the same level. 48.4% of the embryos exhibited severe abnormalities (Fiallos-Oliveros and Ohshima, 2020) and, among them, I observed three main types of phenotypes [Fig. 12 (D-F)]. In the most common two types, a major number of neurons were located in the r4 and r5 regions [Fig. 12 (D, F)]; however, in one of them it was more difficult to differentiate the left and right sides [Fig. 12 (D)]. The third and less frequent group of severely affected embryos corresponds to the ones with an immature-like pattern. In these samples, two separated thin-rows of facial motor neurons and smaller trigeminal nucleus were observed. This pattern was more similar to the one typically found at 28 hpf instead of the one expected at 50 hpf [Fig. 12 (E)]. In addition to this, 29.0% of the samples exhibited milder abnormalities; in these cases, most of the neurons were located at r6, but there were still some groups of neurons that had not completed the migration process or were ectopically located [Fig. 12 (B, C)].

The same region was observed at 72 hpf. At this time, abnormalities in the migration process were also observed [Fig. 13], but the rate was much lower (33.3%; n= 12) compared to the earlier stage of 50 hpf.

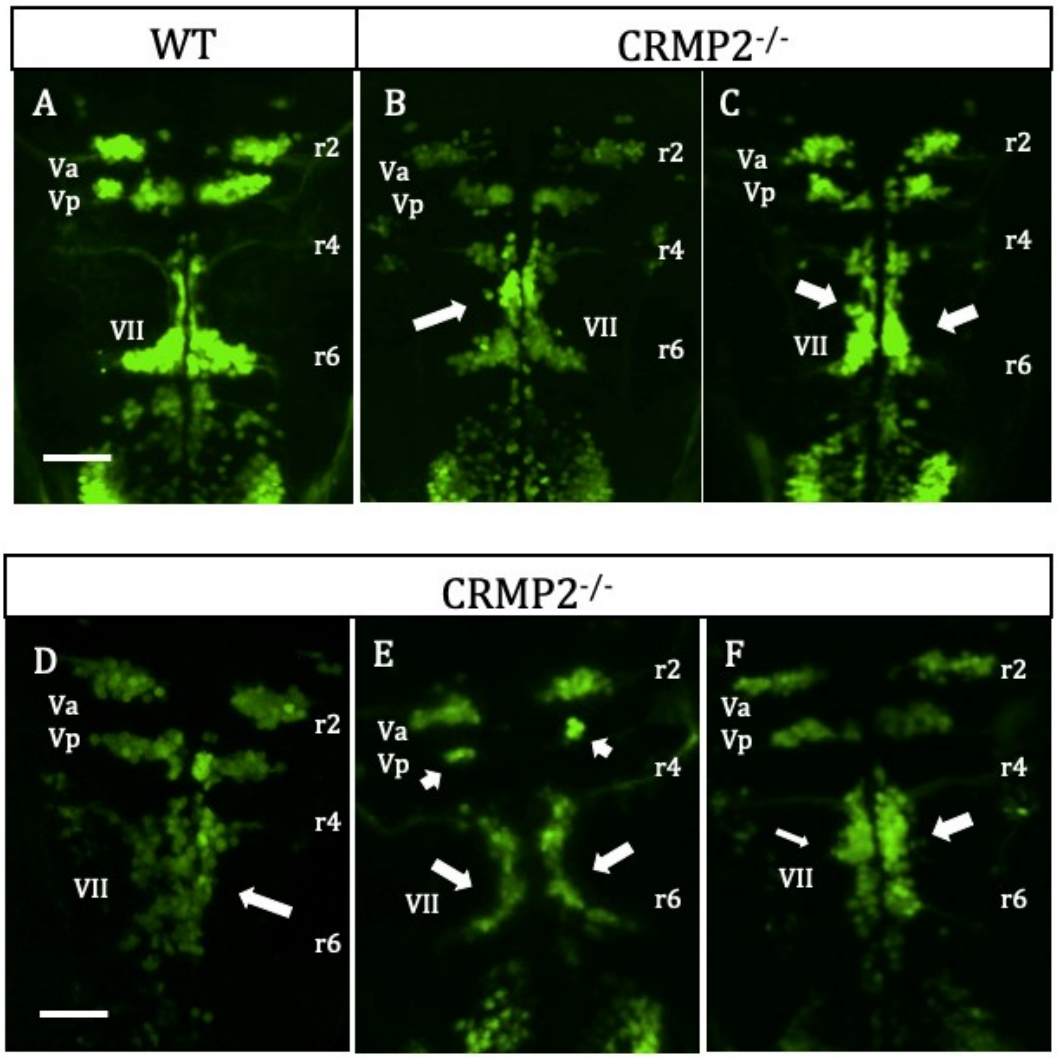

Figure 12. Dorsal view of the cranial motor neurons of WT (A) and CRMP2 KO mutants (B-F) at 50 hpf. In WT embryo most facial (VII) neurons are located at r6. Mutants exhibit different degrees of abnormalities. B, C) Examples of phenotypes with mild abnormalities: in these samples many neurons have completed the migration process, however, the structure does not look completely WT-like. Some groups of neurons are abnormally located, but the phenotype is not as severe as in other embryos. D-E) Phenotypes exhibiting severe abnormalities: there are three main types of severe phenotypes with a different distribution of the facial motor neurons, however, all of them show a decrease in the number of neurons in r6. Abnormal regions are indicated with arrows. Anterior is up. Scale bars= 50 μm.

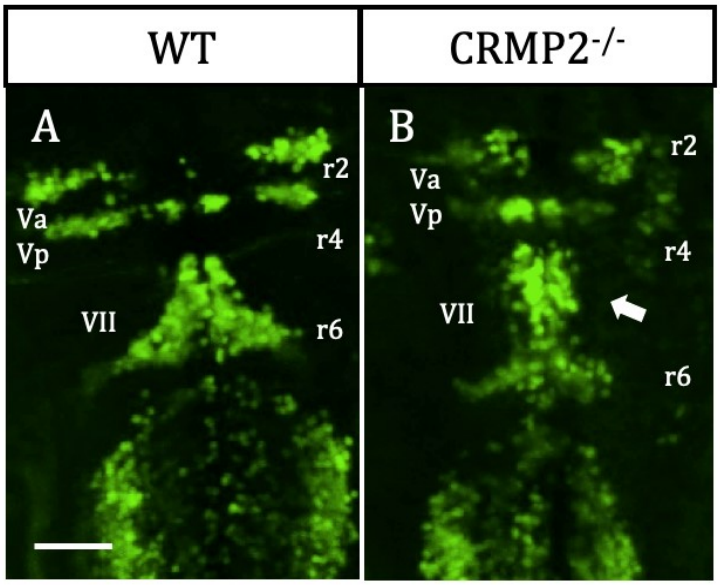

Figure 13. Dorsal view of the cranial motor neurons of WT (A) and CRMP2 KO (B) at 72 hpf. In mutants, neurons tend to remain in the anterior region instead of migrating caudally. Abnormally located neurons are indicated with an arrow. Anterior is up. Scale bar= 50 μm.

3.2.6 CRMP2 knock-out affects the growth of the trigeminal axons

CRMP2 KO; islet1-GFP embryos were observed ventrally at 58 hpf to confirm possible defects in the axonal growth. Deficiencies were observed in 52.2% of the embryos (n= 23). Trigeminal axons of KO embryos extended longer than the axons of the AMO-injected embryos. However, most of them looked thinner and tended to misproject or bifurcate hindering their union in the midline [Fig. 14 (B)]. Here I counted as severely affected all the samples with clear misprojections and as slightly affected the ones with thin axons that did not reach the midline.

Mutants were also fixed at 72 hpf, however, no clear differences were observed compared to the WT [Fig. 14 (C, D)].

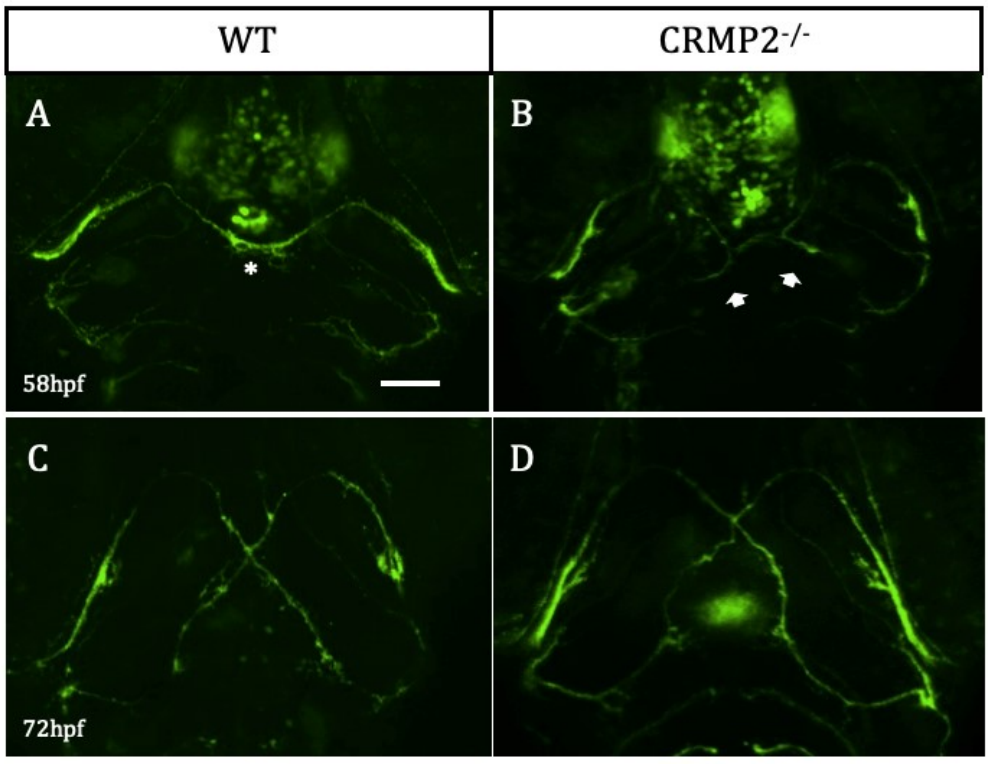

Figure 14. Ventral view of WT and mutant embryo at 58 hpf (A, B) and 72 hpf (C, D). Trigeminal axons failed to cross the midline in the mutant embryo by 58 hpf. Abnormally bifurcating axons are indicated with arrows. The midline is indicated with a star. At 72 hpf clear differences are not observed between WT and mutant samples. Anterior is up. Scale bar= 50 μm.

3.2.7 Analysis of the off-target effects

To analyze whether there had been off-target effects, descendants of heterozygous fish that did not carry the specific mutant sequence were also studied. I refer to these samples as CRMP2$^{+/+}$ to make a difference with the WT embryos descending from WT lines.

CRMP2$^{+/+}$ samples were fixed at 50 hpf and observed dorsally. From the observed embryos (n= 22), 63.6% exhibited WT-like patterns. The remaining samples expressed some degree of abnormalities in the facial nucleus region (Fiallos-Oliveros and Ohshima, 2020).
CRMP2$^{+/+}$ samples were also observed at 58 hpf. At this time point, 87.5% (n= 8) of the embryos exhibited WT like patterns; trigeminal axons extended ventrally until they connected each other in the midline region.

3.2.8 Rescue experiments

CRMP2 KO mutant embryos were injected with different concentrations of CRMP2 mRNA (20, 50 and 100 ng/µl) during the 1 to 2 cell stage in order to rescue the abnormalities observed after the knock-out and prove that the loss of function of CRMP2 was the cause of these abnormalities (Fiallos-Oliveros and Ohshima, 2020).

CRMP2 mRNA injected and uninjected mutants were fixed at 50 hpf to observe dorsally the migration process of the facial motor neurons. Among the embryos injected with 100 ng/µl of CRMP2 mRNA (n= 23), 56.5% expressed a WT-like pattern; most of the facial motor neurons were located at r6 by 50 hpf [Fig. 15 (C)]. After injecting lower concentrations of CRMP2 mRNA the percentage of rescued embryos was also lower: 36.4% of the mutant embryos injected with 50 ng/µl of CRMP2 mRNA (n= 11) and 31.3% of the ones injected with 20 ng/µl (n= 16) exhibited WT-like patterns, indicating a dose dependency. These results support a role of CRMP2 in the migration of the facial motor neurons (Fiallos-Oliveros and Ohshima, 2020).

In addition, a few (n= 6) of the CRMP2 KO mutant embryos injected with CRMP2 mRNA (100 ng/µl) were fixed at 58 hpf to confirm the rescue in the elongation of the trigeminal axons. In this case, 50% of the embryos exhibited a clear WT-like pattern [Fig. 15 (D)].

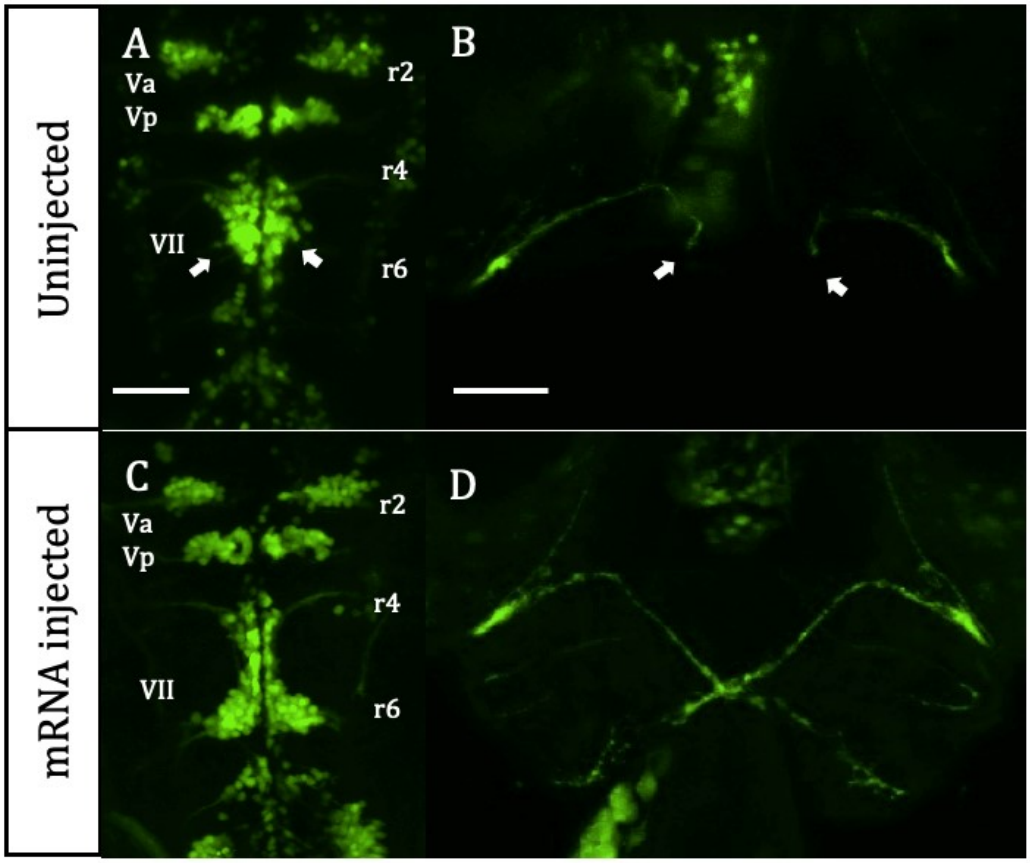

Figure 15. Dorsal view at 50 hpf (A, C) and ventral view at 58 hpf (B, D) of the cranial motor neurons of CRMP2 KO mutant embryos injected with 100 ng/µl of CRMP2 mRNA (C, D) and uninjected (A, B). The uninjected embryo shows clear defects in both the migration of facial motor neurons (VII) and the elongation of trigeminal axons. The CRMP2 mRNA injected embryo exhibited a WT-like pattern in both the migration of facial motor neurons and the elongation of trigeminal axons. Anterior is up. Scale bars= 50 µm. Modified from Fiallos-Oliveros and Ohshima, 2020.

3.2.9 Data analysis

At 50 hpf, 77.4% of the mutant embryos (n= 31) expressed some degree of abnormalities in the caudal migration of the facial motor neurons. However, 36.3% of the CRMP2$^{+/+}$ (n= 22) and 43.5% of the CRMP2 mRNA (100 ng/µl) injected mutants (n= 23) also expressed some kind of abnormalities. To confirm whether the differences between the percentage of abnormal phenotypes in homozygotes embryos and the other groups were statistically significant I performed a chi-squared test. I compared the frequency of WT-like, slightly affected, and severely affected phenotypes between the groups (Fig. 16). The chi-squared test and subsequent post hoc analysis indicated that, although the percentage of slightly affected embryos was similar between the three groups, the proportion of samples with a severe phenotype was significantly different in the KO mutants. In the same way, the number of samples expressing a WT-like phenotype was significantly different in mutants compared to the other two groups. These analyses support a relationship between the CRMP2$^{-/-}$ genotype and the increase of abnormal samples; in other words, that CRMP2 has a role in the migration of the facial motor neurons (Fiallos-Oliveros and Ohshima, 2020).

At 58 hpf, the number of CRMP2$^{+/+}$ (n= 8) and CRMP2 mRNA injected CRMP2$^{-/-}$ samples (n= 6) was low compared to the other groups. Therefore, in order to make a meaningful comparison, I contrasted the proportion of WT- like, slightly abnormal, and severely affected phenotypes between WT samples (n= 19) and those in the mutants (n= 23). In this case, the chi-squared test indicated significant differences between the frequencies of abnormal samples observed in each group [Fig. 16 (B)]. Therefore, it confirms that the increase in the number of abnormal samples is related to the mutation.

A) Percentage of samples with WT-like and abnormal phenotype at 50hpf

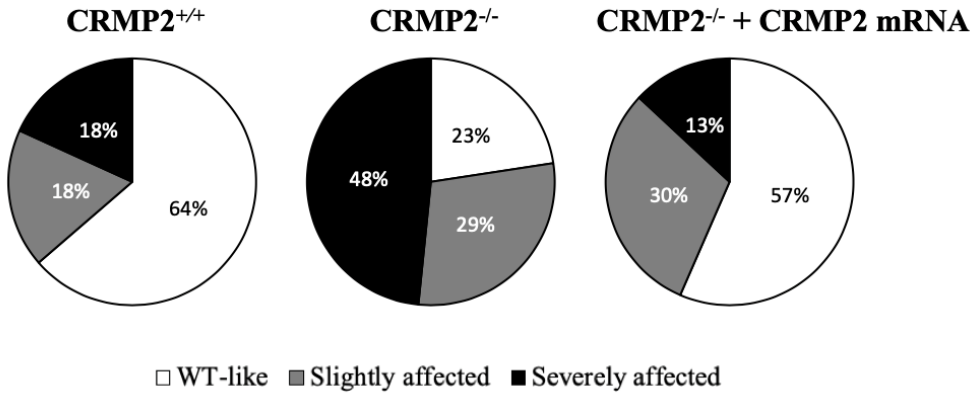

B) Percentage of samples with WT-like and abnormal phenotype at 58hpf

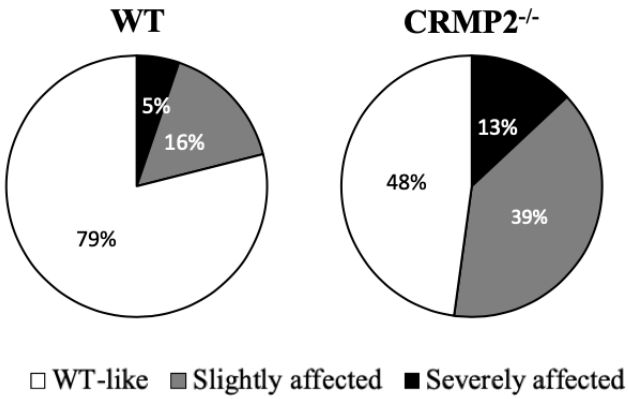

Figure 16. Percentage of abnormal samples in the different groups analyzed.

(A) Percentage of WT-like and abnormal phenotypes (severely and slightly affected) observed in the facial motor neurons migration of CRMP2$^{+/+}$ (n= 22), CRMP2$^{-/-}$ (n= 31) and CRMP2 mRNA injected (100 ng/µl) CRMP2$^{-/-}$ (n= 23) at 50 hpf. X^2 (4)= 13.598, p= 0.009< 0.05; indicates differences between the groups. For the post hoc analysis, a new P-value of 0.005 was established; this one determined that the number of WT-like and severely affected samples identified in the KO group is significantly different compared to the ones in the other groups with $p < 0.005$ (Fiallos-Oliveros and Ohshima, 2020).

(B) Percentage of WT-like and abnormal phenotypes (severely and slightly affected) observed in WT (n= 19) and CRMP2$^{-/-}$ (n= 23) regarding the elongation of trigeminal axons at 58 hpf. $X^2(1)$= 4.273, p= 0.039< 0.05; there are significant differences between these two groups.

3.2.10 DiI injection

Previous studies that used morpholino mediated knock-downs showed a role of CRMPs in the growth and guidance of the retinal axons (Liu et al., 2018). To elucidate whether a CRMP2 KO causes similar defects as observed in the knock-down, I injected DiI into the right eye of 4 dpf CRMP2 KO larvae and observed the projection of the labeled retinal axons.

Preliminary results did not show a dramatic decrease in the retinal axon growth or abnormalities in the axonal guidance. However, in approximately 55.5% of the observed CRMP2 $^{-/-}$ larvae (n= 17) the retinal axons looked thinner compared to CRMP2 $^{+/+}$ or WT axons (Fig. 17). Although the phenotype observed was not as severe as shown in previous research where morpholinos were used, these results could support the involvement of CRMP2 in the growth of retinal axons.

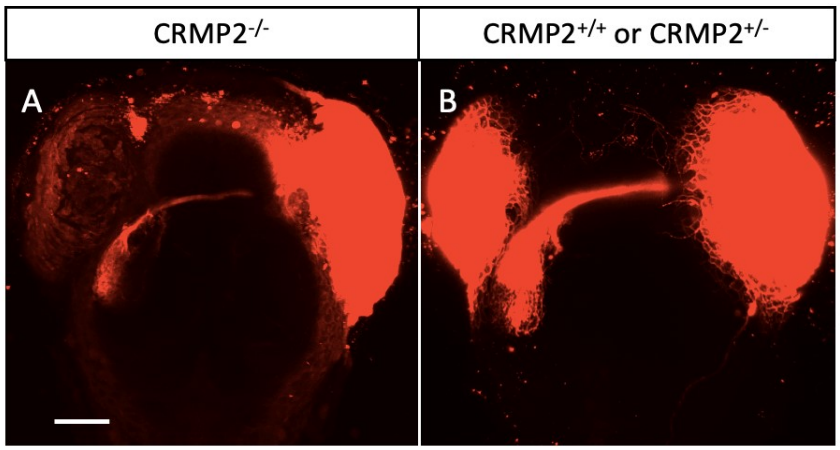

Figure 17. Retinal axons of (A) CRMP2 $^{-/-}$ and (B) CRMP2 $^{+/+}$ or CRMP2 $^{+/-}$ embryos injected with DiI. Misprojections in the axonal guidance are not observed, but the axonal growth could be slightly decreased in the KO mutant. Anterior is up. Scale bar= 100 μm.

Chapter 4: Discussion

The role of CRMPs in axonal growth and cell migration in the nervous system has been well studied in different species. The role of CRMP2 has also been studied in zebrafish to understand better its functions *in vivo*. However, here I used different means to show for the first time the involvement of this protein in the migration and axonal elongation of the cranial motor neurons in zebrafish. On the one hand, I knocked down the gene using morpholino oligonucleotides, but I also generated a CRMP2 KO line thanks to the CRISPR/Cas9 technology.

4.1 Generation of a CRMP2 KO mutant line

I faced some difficulties trying to establish a CRMP2 KO mutant line, especially due to the high death rate of the offspring of the homozygous fish. However, I found a specific mutation that disrupted the gene as I intended and allowed the study of different processes in which CRMP2 could be involved.

I generated a CRMP2 mutant line that could be used for the study of different roles of CRMP2, not only in brain development. Mutant embryos did not exhibit obvious abnormalities regarding general morphology or behavior. Even though it is difficult to keep as a homozygous line and their lifespan might be shorter than WT fish, KO fish can be easily obtained from heterozygous parents and a big part of them will reach adulthood; therefore, this line is also useful for studies at different stages.

Figure 18. Comparison between WT and CRMP2$^{-/-}$ embryos at 2 dpf in lateral view. CRMP2$^{-/-}$ has no pigmentation due to 1-phenyl-2-thiourea treatment. Anterior is on the left. Dorsal is up. Scale bar= 500 μm.

4.2 CRMP2 is required for the proper migration of the facial motor neurons during early development

My studies using both AMOs and CRISPR/Cas9 system show that CRMP2 has a role in the migration of facial motor neurons during the development of the zebrafish nervous system. During normal development, facial motor neurons migrate progressively from r4 and r5 to r6 and r7 and most of these neurons have reached their location in r6 and r7 by 36 hpf (Higashijima et. al, 2000). I waited until 50 hpf to observe the CRMP2 AMO injected and CRMP2 mutant embryos, a time when most of the facial motor neurons should be already at the caudal region of the facial nucleus. However, even at this time, I observed abnormalities in the positioning of these neurons.

The phenotype induced by AMO injection was similar in all cases, independently of the concentration. In the morphants, most of the cells were accumulated between r5 and r6 differing from the usual distribution of the facial motor neurons. When the translation blocking AMO was injected, the phenotype observed was more severe, probably due to a higher efficiency inhibiting the production of CRMP2 protein. Translation blocking AMOs bind to the post-spliced mRNA (both maternal and zygotic mRNA) and block the progression of the ribosomal initiation complex; splicing blocking AMOs block the proper processing of pre-mRNA (Eimon, 2014), they do not affect the maternal mRNA. Therefore, it could be that the phenotype induced by the splicing blocking AMO was less severe than the induced by the translation blocking AMO because of the protein produced by the maternal mRNA. The phenotypes observed in CRMP2 KO mutants were more diverse, but they were affecting the same region (Fiallos-Oliveros and Ohshima, 2020).

The possibility of developmental defects instead of migration defects was also considered. One the one hand, I did not observe evident morphological or general abnormalities in the mutants. Some embryos were slightly bending, but that situation can occur also with WT fish. Interestingly, even when the general morphology was similar and apparently WT-like in the mutants, differences in the distribution of the facial motor neurons were observed (Fig. 19).

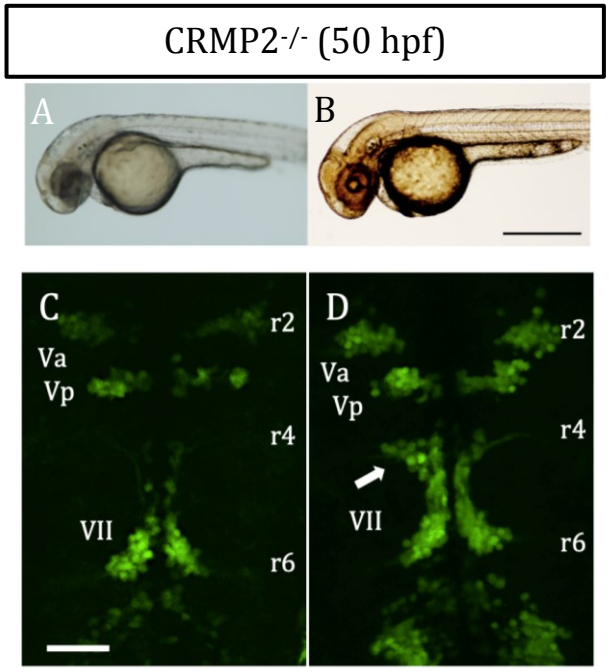

Figure 19. A, B) Bright-field images of CRMP2$^{-/-}$ embryos apparently WT-like seen laterally. Anterior is on the left. Scale bar= 500 μm. C, D) Dorsal view of the cranial motor neurons of fish A and B respectively. In C most of neurons are located at r6; in D a group of neurons are still at r4 (indicated with an arrow). Anterior is up. Scale bar= 50 μm.

On the other hand, I decided to observe some embryos at 28 hpf, let them grow, and fix them at 50 hpf for phenotype observation. At 28 hpf most of the embryos exhibited similar patterns irrespective of the genotype. However, at 50 hpf some of them manifested defects in the location of the facial motor neurons (Fig. 20).

This point could be further studied by analyzing more embryos at earlier times in vivo, checking the location of the facial motor neurons at more stages to detect when the defects begin to appear. In addition, it would be interesting to observe if at some later point the neurons end up finding their expected location. In my research I found a greater percentage of abnormalities at earlier stages (50 hpf) if compared with 72 hpf. It would be good to determine if these observations are due to a delayed migration or if most of the severely affected samples died before 72 hpf.

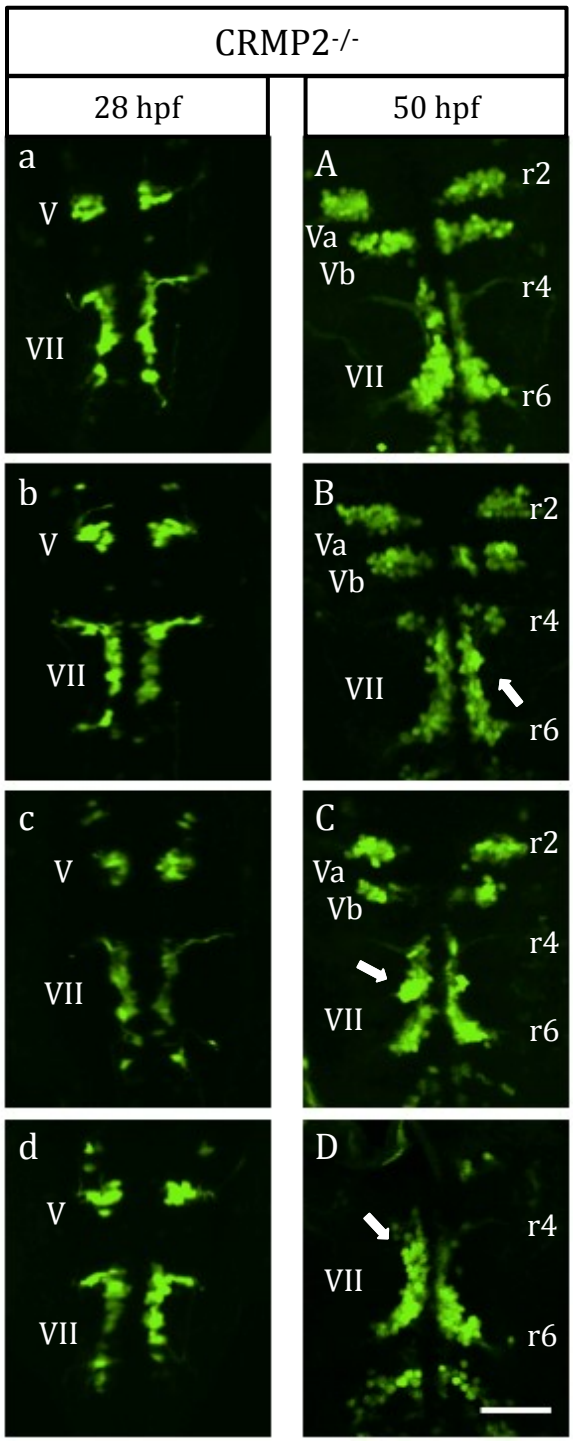

Figure 20. Dorsal view of CRMP2$^{-/-}$ cranial motor neurons at 28 (left) and 50 hpf (right). At 28 hpf, the facial nucleus (VII) exhibits two thin rows of neurons. By 50hpf, the trigeminal nucleus (V) has already divided into anterior (Va) and posterior (Vp) and most of the facial motor neurons are expected to be at r6 as in sample A. Although there are no big differences at the stage of 28hpf, there are some abnormalities (arrows) in the location of the motor neurons at 50 hpf, suggesting defects in the migration process. In all images anterior is up. Scale bar= 50 μm.

These observations clarify that the abnormalities observed were not due to developmental defects, but related to a role of CRMP2 in the migration of facial motor neurons.

These analyses, using both morpholino-induced knock-down and CRMP2 KO mutants, let me assess that CRMP2 has a role in the migration of the cranial motor neurons during the development of the zebrafish nervous system. This finding is consistent with previous researches that indicate a role of Nrp1 (neuropilin 1) and the semaphorin Sema3A in the patterning of the facial nerve in mice (Schwarz et al., 2004).

4.3 CRMP2 is required for the proper elongation of the trigeminal axons during early development

Previous studies in mice have shown an involvement of semaphorins in axonal projection in both cranial and spinal neurons (Kitsukawa et al., 1997). Besides, other studies in zebrafish indicated a requirement of Sema3a1/Plxna3 signaling for the proper axonal pathfinding of the posterior trigeminal and facial motor neurons (Tanaka et al., 2007).

CRMP2 is known for mediating in the semaphorin signaling pathway and this research indicates that CRMP2 is involved in the proper elongation of the trigeminal axons during nervous system development. By 58 hpf, posterior trigeminal axons are expected to have extended ventrally and to be crossing the midline. However, the axons of CRMP2 mutants extended abnormally, frequently failing to reach the midline. In the knock-down experiments, morphants exhibited a more severe phenotype as if they were in the early stages of elongation. Although knock-out and knock-down induced different phenotypes, it is clear that CRMP2 is necessary for the proper elongation of these axons, at least during their early development. CRMP2 KO samples observed at 72 hpf exhibited WT-like patterns, which make it likely to think that other genes are taking the role of CRMP2 allowing axons to complete their extension. In addition, the phenotype observed in CRMP2 morphants is different from the ones observed in Sema3a1 or Plxna3 morphants previously, indicating that there are other genes involved in the proper axonal elongation of cranial motor neurons.

4.4 It is not likely that the phenotype is due to off-target effects

During these studies, I also analyzed the descendants from the heterozygous fish that did not carry the specific mutation identified in order to deny possible off-target effects. I identified them as CRMP2$^{+/+}$ to make a difference between them and the WT fish descending from WT parents.

63.6% of the CRMP2$^{+/+}$ samples fixed at 50 hpf and observed dorsally (n= 22) exhibited WT-like patterns [Fig. 21 (C)]. In the remaining samples I found abnormalities of some degree as I did in 20.0% of WT embryos (n= 35) (Fiallos-Oliveros and Ohshima, 2020). On the other hand, 12.5% of the CRMP2$^{+/+}$ samples observed at 58 hpf (n= 8) expressed clear abnormalities, at this time point most of the embryos exhibited WT-like patterns; trigeminal axons extended ventrally until they connected each other in the midline region [Fig. 21 (D)]. Similarly, 21.0% of the WT samples exhibited some abnormalities at this time.

A chi-square test was performed for statistical analysis between the CRMP2$^{+/+}$ and the WT group. The results show that the frequencies of WT-like and abnormal samples observed both at 50 and 58 hpf in the CRMP2$^{+/+}$ were not significantly different compared to the WT ones [Fig. 21 (D, E)]. The CRMP2$^{+/+}$ group was also compared to the homozygous mutants and the results determined that the frequencies were significantly different between them. Therefore, these results indicate that, in both the migration of facial motor neurons and the elongation of trigeminal axons, the high percentage of abnormal samples in the CRMP2$^{-/-}$ is related to the mutation, not an off-target effect (Fiallos-Oliveros and Ohshima, 2020).

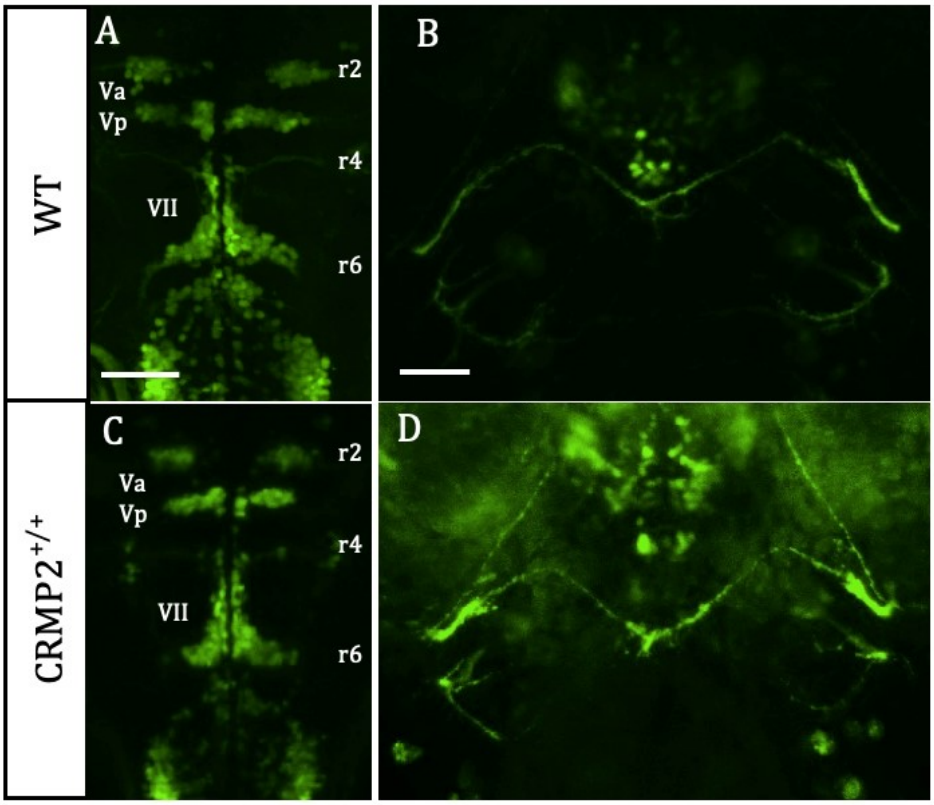

E) Percentage of samples with WT-like and abnormal phenotype at 50hpf

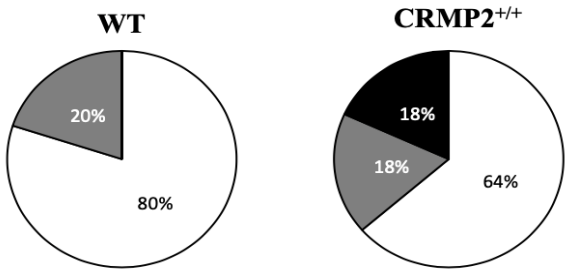

F) Percentage of samples with WT-like and abnormal phenotype at 58hpf

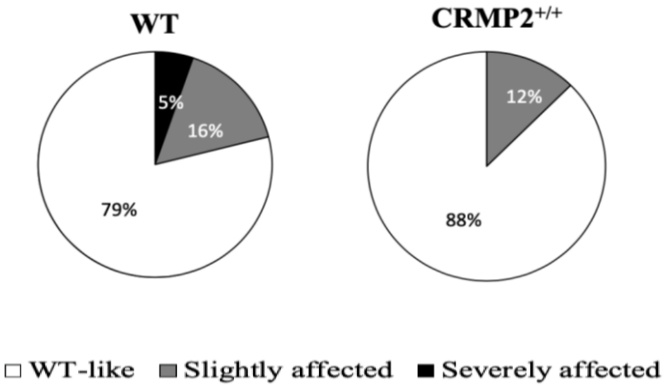

Figure 21. A, C) Dorsal view of the cranial motor neurons at 50 hpf. B, D) Ventral view of the cranial region at 58 hpf. CRMP2$^{+/+}$ embryo exhibits a proper migration pattern in the facial nucleus (VII) at 50 hpf and its trigeminal axons have extended ventrally the same way they extend in WT. Anterior is up. Scale bars= 50 μm. E) Graphs comparing the percentage of WT-like and abnormal samples between WT (n= 35) and CRMP2$^{+/+}$ (n= 22) embryos observed at 50 hpf (modified from Fiallos-Oliveros and Ohshima, 2020). $X^2(1)= 1.865$, p= 0.172>0.05; there are no significant differences between these two groups. F) Graphs comparing the percentage of WT-like and abnormal samples between WT (n= 19) and CRMP2$^{+/+}$ (n= 8) embryos at 58 hpf. $X^2(1)= 0.273$, p= 0.6>0.05; there are no significant differences between these groups.

4.5 Discrepancies between KO and KD phenotypes

In this research, I also analyzed whether the phenotypes induced by CRMP2 KO and KD were similar. At first, I tried to observe the positioning of the caudal primary motor neurons in the spinal cord at 28 hpf. Unexpectedly, in any of the mutant samples clear abnormalities were found. Technical difficulties made it hard to increase the number of analyzed samples. It is possible that like in the cranial motor neurons migration and axonal elongation, not all the samples exhibit a clear phenotype; therefore, if the number of samples is low it may be more difficult to detect deficiencies. However, it is also likely that other genes, probably other CRMP family members, could be compensating the lack of CRMP2 in the KO mutants and for that reason I did not see a phenotype.

It is known that in some situations a gene knock-out triggers the upregulation of other genes and proteins (Rossi et al., 2015). The compensatory mechanisms that are activated due to genetic ablation are not present when the genome is not altered (Rossi et al., 2015; Zimmer et al., 2019). This is a possible explanation for the lack of phenotype in the CRMP2 KO mutants, even though Morimura et al. (2013) proved the role of CRMP2 in the positioning of the caudal primary motor neurons in the spinal cord.

A similar situation occurred with the growth of the retinal axons. Liu et al. (2018) described a severe reduction in the axonal growth of CRMP2 morphants that I did not observe in the mutants. I observed thinner axons in a 55.5% of CRMP2 $^{-/-}$ larvae, but not an apparent reduction in the axonal growth as they did. The differences I observed between CRMP2$^{-/-}$ and WT or CRMP2$^{+/+}$ could be due to technical skills. However, CRMP2$^{+/+}$ and WT larvae were injected under the same conditions, and here only 25% of the samples exhibited thinner retinal axons. It is more likely that compensatory mechanisms are activated due to the lack of CRMP2 and lead to the attenuation of the phenotype expression.

In the migration process of the cranial motor neurons some differences between mutants and morphants were also observed. The morphant phenotype was more severe and constant than the mutant one (Fiallos-Oliveros and Ohshima, 2020).

Similarly, trigeminal axon elongation was strongly affected by the knock-down, while knock-out embryos exhibited more diversity in their phenotypes. In both situations, CRMP2 mutants expressed a variability that could be dependent both on the level of penetrance and expression of the mutation or on the degree of compensation by other genes. It is known that CRMP family members have similar roles and some of them could be compensating the CRMP2 loss of function in the mutants (Fiallos-Oliveros and Ohshima, 2020). It would be good to study if there is an upregulation of any of them in the CRMP2$^{-/-}$ fish.

Another possible explanation for the discrepancies in the phenotypes in knock-down and knock-out experiments could be the presence of maternal WT mRNA in the mutants (Zimmer *et al.* 2019). The presence of maternal mRNA in the descendants of CRMP2$^{+/-}$ fish could mitigate the effects of the knock-out, as it might be happening in the case of splicing blocking AMO injected embryos (Fiallos-Oliveros and Ohshima, 2020).

All these comparisons point out some differences between the knock-out and the knock-down phenotypes. However, these differences do not invalidate the hypothesis that CRMP2 has a role in all these processes during development.

Chapter 5: Future prospects

5.1 Analysis of other CRMP2 KO lines

I generated a mutant line in which a nucleotide insertion disrupted CRMP2 gene, and found some abnormalities in the development of the cranial motor neurons. To confirm these findings, it would be good to study other CRMP2 KO lines with a different mutant sequence generated either with the CRISPR/Cas9 system or other methods. If the same phenotype is observed, this will strongly support the role of CRMP2 in the migration of facial motor neurons and the elongation of trigeminal axons.

In parallel with the CRISPR/Cas9 generated CRMP2 KO line, I have been growing a CRMP2 mutant line that I got from the Sanger Institute. This line consists of just a 1bp change, sufficient to truncate its sequence. This would be a good line to perform a similar study and prove the findings in the current one.

5.2 Generation of a CRMP double KO line

CRMP family members are expressed in similar regions throughout the nervous system and some of them accomplish similar roles. Previous studies have shown similar effects after knocking down CRMP2 and CRMP4; therefore, CRMP4 or other CRMP family members might be compensating the lack of CRMP2 in the knock-out mutants. This would explain why I did not see clear abnormalities in the positioning of the caudal primary motor neurons in the spinal cord, for example. Therefore, as one of the next steps to this research, it would be interesting to generate a CRMP4 KO line in zebrafish and analyze its effects in facial motor neuron migration and trigeminal axon elongation and subsequently study the same processes in the CRMP2; CRMP4 double KO line. It is possible that knocking out different CRMPs at the same time helps to elucidate how these proteins work.

5.3 Study the role of CRMPs in the fin regeneration of adult zebrafish

During this research, I observed defects in the caudal fin regeneration of adult CRMP2 KO mutants. It was not my aim to study the roles of CRMP2 outside the nervous system development; however, as cutting the caudal fin of the fish was necessary to extract genomic DNA from adult fish and carry out the experiments, it was inevitable to observe the differences once it regenerated.

Usually, after a cut, zebrafish caudal fin regenerates, achieving its original emarginate shape with three blue stripes in a few weeks. However, in many of the CRMP2 mutants, I observed changes in their caudal fin after regeneration. Weeks after the caudal fin was cut, I realized that most of the CRMP2 KO adult fish expressed abnormalities in the shape or pigmentation of the caudal fin that were absent originally. KO mutants frequently had a squared or slightly truncated fin after regeneration and it was not unusual to find fins with very short stripes or almost transparent fins. These features were not typically observed in $CRMP2^{+/+}$ or $CRMP2^{+/-}$ fish after regeneration; therefore, this characteristic made it easier to identify KO fish. Preliminary results are shown in figure 22.

Previous studies indicate that semaphorins and plexins are involved in the regeneration of zebrafish fin (Ton and Iovine, 2012; Pfefferli and Jazwinska, 2015). Knowing that semaphorins and plexins interact with CRMP2 during nervous system development, it would not be surprising that these molecules are working similarly in the regeneration process. The signaling pathway involving semaphorins and CRMPs might not be restricted only to the nervous system. Therefore, fin regeneration would be an interesting process in which to study the functions of CRMP2.

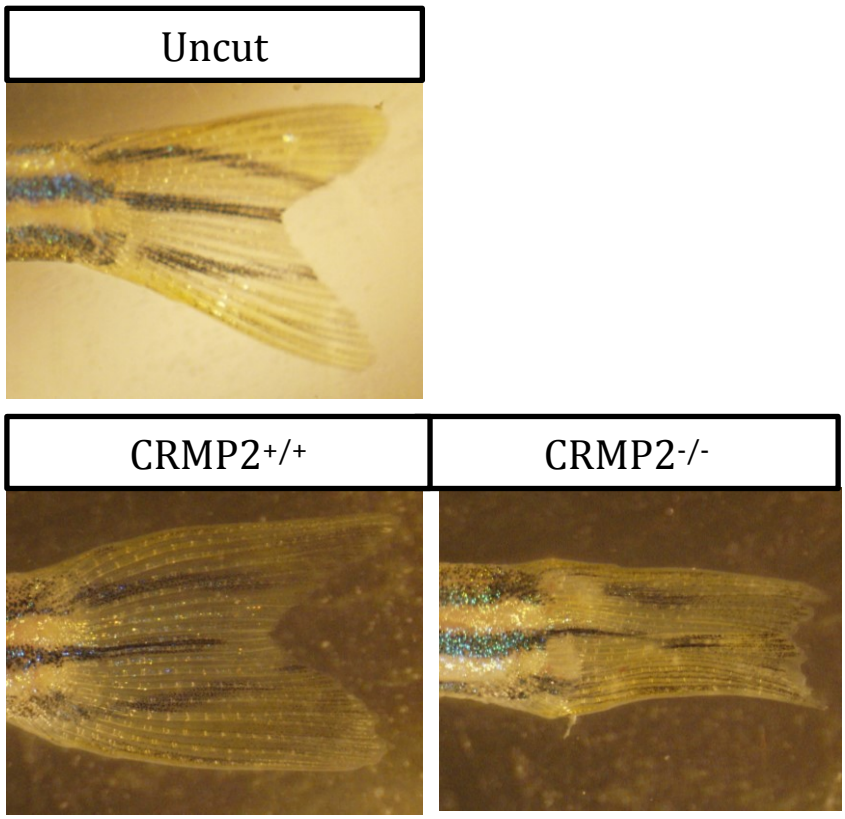

Figure 22. Lateral view of the caudal fin of adult zebrafish. (A) Uncut fin of a heterozygous x heterozygous descendant; fin with a WT shape. (B, C) Fins of CRMP2$^{+/+}$ and CRMP2$^{-/-}$ adult fish after regeneration. CRMP2$^{+/+}$ samples regenerated fins normally, KO mutants exhibit a different pattern.

References

Beasley, T.M. and Schumacker, R.E. (1995). Multiple Regression Approach to Analyzing Contingency Tables: Post Hoc and Planned Comparison Procedures. The Journal of Experimental Education, 64(1):79-93.

Christie, T.L., Starovic-subota, O., Childs, S. (2006). Zebrafish collapsin response mediator protein (CRMP)-2 is expressed in developing neurons. Gene Expression Patterns, 6(2):193-200.

Crooke, S. T. (1996). Progress in antisense therapeutics. Medicinal Research. Reviews, 16(4):319-344.

Cong, L., Ran, F.A., Cox, D., Lin, S., Barretto, R., Habib, N., Hsu, P.D., Wu, X., Jiang, W., Marraffini, L.A., Zhang, F. (2013). Multiplex genome engineering using CRISPR/Cas systems. Science, 339(6121):819-823.

Culverwell, J. and Karlstrom, R.O. (2002). Making the connection: retinal axon guidance in the zebrafish. Seminars in cell & developmental biology, 13(6):497-506.

Eimon, P.M., (2014). Studying apoptosis in the Zebrafish. Methods in Enzymology, 544(16):395-431.

Fiallos Oliveros, C. and Ohshima, T. Dpysl2 (CRMP2) is required for the migration of facial motor neurons in developing zebrafish embryos. The International Journal of Developmental Biology, *in press.*

Gaj, T., Gersbach, C.A., Barbas, C.F. 3rd. (2013). ZFN, TALEN, and CRISPR/Cas-based methods for genome engineering. Trends in Biotechnology, 31(7):397-405.

Gong, C., Bongiorno, P., Martins, A., Stephanou, N.C., Zhu, H., Shuman, S., Glickman, M.S. (2005). Mechanism of nonhomologous end-joining in mycobacteria: a low-fidelity repair system driven by Ku, ligase D and ligase C. Nature Structural & Molecular Biology, 12(4):304-312.

Goshima, Y., Nakamura, F., Strittmatter, P., Strittmatter, S.M. (1995). Collapsin-induced growth cone collapse mediated by an intracellular protein related to UNC-33. Nature, 376(6540):509-514.

Higashijima, S., Hotta, Y., Okamoto, H. (2000). Visualization of cranial motor neurons in live transgenic zebrafish expressing green fluorescent protein under the control of the islet-1 promoter/enhancer. The Journal of Neuroscience, 20(1):206-218.

Howe, D.G., Bradford, Y.M., Conlin, T., Eagle, A.E., Fashena, D., Frazer, K., Knight, J., Mani, P., Martin, R., Taylor Moxon, S.A., Paddock, H., Pich, C., Ramachandran, S., Ruef, B.J., Ruzicka, L., Schaper, K., Shao, X., Singer, A., Sprunger, B., Van Slyke, C.E., Westerfield, M. (2013). ZFIN, the Zebrafish Model Organism Database: increased support for mutants and transgenics. Nucleic acids research, 41(D1):D854-860.

Hruscha, A., Krawitz, P., Rechenberg, A., Heinrich, V., Hecht, J., Haass, C., Schmid, B. (2013). Efficient CRISPR/Cas9 genome editing with low off-target effects in zebrafish. Development, 140(24):4982-4987

Karlstrom, R.O., Trowe, T., Klostermann, S., Baier, H., Brand, M., Crawford, A.D., Grunewald, B., Haffter, P., Hoffman, H., Meyer, S.U., Muller, B.K., Richter, S., van Eeden, F.J., Nüsslein-Volhard, C., and Bonhoeffer, F. (1996). Zebrafish mutations affecting retinotectal axon pathfinding. Development, 123(1):427-438.

Kimmel, C.B., Warga, R.M., Schilling T.F. (1990). Origin and organization of the zebrafish fate map. Development, 108(4):581-594.

Kimmel, C.B., Warga, R.M., and Kane, D.A. (1994). Cell cycles and clonal strings during formation of the zebrafish central nervous system. Development, 120(2):265-276.

Kimmel, C.B., Ballard, W.W., Kimmel, S.R., Ullmann, B., Schilling, T.F. (1995). Stages of embryonic development of the zebrafish. Developmental Dynamics, 203(3):253–310.

Kitsukawa, T., Shimizu, M., Sanbo, M., Hirata, T., Taniguchi, M., Bekku, Y., Yagi, T. and Fujisawa, H. (1997). Neuropilin-Semaphorin III/D-mediated chemorepulsive signals play a crucial role in peripheral nerve projection in mice. Neuron, 19(5):995-1005.

Kok, F.O., Shin, M., Ni, C., Gupta, A., Grosse, A.S., van Impel, A., Kirchmaier, B.C., Peterson-Maduro, J., Kourkoulis, G., Male, I., DeSantis, D.F., Sheppard-Tindell, S., Ebarasi, L., Betsholtz, C., Schulte-Merker, S., Wolfe, S.A., Lawson, N.D. (2015). Reverse Genetic Screening Reveals Poor Correlation between Morpholino-Induced and Mutant Phenotypes in Zebrafish. Developmental Cell, 32(1):97-108.

Kotani, H., Taimatsu, K., Ohga, R., Ota, S., Kawahara, A. (2015). Efficient Multiple Genome Modifications Induced by the crRNAs, tracrRNA and Cas9 Protein Complex in Zebrafish. PLoS One, 10(5):e0128319.

Lele, Z., Krone, P.H. (1996). The zebrafish as a model system in developmental, toxicological and transgenic research. Biotechnology Advances, 14(1):57-72.

Liu, Z.Z., Zhu, J., Wang, C.L., Wang, X., Han, Y.Y., Liu, L.Y., Xu, H.A. (2018). CRMP2 and CRMP4 Are Differentially Required for Axon Guidance and Growth in Zebrafish Retinal Neurons. Neural Plasticity, 2018:8791304.

Morimura, R., Nozawa, K., Tanaka, H., Ohshima, T. (2013). Phosphorylation of Dpsyl2 (CRMP2) and Dpsyl3 (CRMP4) is required for positioning of caudal primary motor neurons in the zebrafish spinal cord. Developmental Neurobiology, 73(12):911-920.

Nasevicius, A., Ekker, S.C. (2000). Effective targeted gene 'knockdown' in zebrafish. Nature Genetetics, 26(2):216-220.

Reis, A., Hornblower, B., Robb, B., Tzertzinis, G. (2014). CRISPR/Cas9 and Targeted Genome Editing: A New Era in Molecular Biology. NEB expressions, 2014(1):3-6.

Rossi, A., Kontarakis, Z., Gerri, C., Nolte, H., Hölper, S., Krüger, M., Stainier, D.Y.R. (2015). Genetic compensation induced by deleterious mutations but not gene knockdowns. Nature, 524(7564):230–233.

Schmidt, E. F. and Strittmatter, S. M. (2007). The CRMP family of proteins and their role in Sema3A signaling. Advances in experimental medicine and biology, 600:1–11.

Schwarz, Q., Gu, C., Fujisawa, H., Sabelko, K., Gertsenstein, M., Nagy, A., Taniguchi, M., Kolodkin, A.L., Ginty, D.D., Shima, D.T., Ruhrberg, C. (2004). Vascular endothelial growth

factor controls neuronal migration and cooperates with Sema3A to pattern distinct compartments of the facial nerve. Genes & Development, 18(22):2822-2834.

Schweitzer, J., Becker, C.G., Schachner, M., and Becker, T. (2005). Expression of collapsin response mediator proteins in the nervous system of embryonic zebrafish. Gene Expression Patterns, 5(6):809-816.

Summerton, J. and Weller, D. (1997). Morpholino antisense oligomers: design, preparation, and properties. Antisense & Nucleic Acid Drug Development, 7(3):187-95.

Tanaka, H., Maeda, R., Shoji, W., Wada, H., Masai, I., Shiraki, T., Kobayashi, M., Nakayama, R., Okamoto, H. (2007). Novel mutations affecting axon guidance in zebrafish and a role for plexin signalling in the guidance of trigeminal and facial nerve axons. Development, 134(18):3259-3269.

Tanaka, H., Morimura R, Ohshima T. (2012). Dpysl2 (CRMP2) and Dpysl3 (CRMP4) phosphorylation by Cdk5 and DYRK2 is required for proper positioning of Rohon-Beard neurons and neural crest cells during neurulation in zebrafish. Developmental Biology, 370(2):223-236.

Ton, Q.V., Kathryn Iovine, M. (2012). Semaphorin3d mediates Cx43-dependent phenotypes during fin regeneration. Developmental Biology, 366(2):195–203.

Wang, L.H., Strittmatter, S.M. (1996). A family of rat CRMP genes is differentially expressed in the nervous system. The Journal of Neuroscience, 16(19):6197-6207.

Westerfield, M. (2000). The zebrafish book. A guide for the laboratory use of zebrafish (Danio rerio). 4th ed., Univ. of Oregon Press, Eugene.

Wiedenheft, B., Sternberg, S.H., Doudna, J.A. (2012). RNA-guided genetic silencing systems in bacteria and archaea. Nature, 482(7385):331-338.

Woo, K., Fraser, S.E. (1995). Order and coherence in the fate map of the zebrafish nervous system. Development, 121(8):2595-2609.

Zimmer, A.M., Pan, Y.K., Chandrapalan, T., Kwong, R.W.M., Perry, S.F. (2019). Loss-of-function approaches in comparative physiology: is there a future for knockdown experiments in the era of genome editing? The Journal of Experimental Biology, 222(7):175737.

Acknowledgments

I would like to express my deep gratitude to Professor Ohshima for his support and supervision throughout all these years. His empathy and constant advice made it easier to carry out this work.

I am also grateful to Professor Inoue for his useful suggestions during the joint seminars, with Professor Campbell for his advice and help with zebrafish experiments and Professor Kubo for her help lending me WT fish, so I could take comparison pictures for the discussion part.

I feel thankful with all Ohshima lab members for making my life in Japan smoother, but I want to especially thank Dr. Shimizu, Mr. Lin and Mr. Ueda for their patience and teachings.

I am sincerely grateful to Otsuka Toshimi Scholarship Foundation for its selfless aid, funding my studies during these years.

Finally, I would like to thank my family for always supporting me both economically and emotionally and my friends for being always encouraging me despite the distance.

List of research achievements

Publications

"Dpysl2 (CRMP2) is required for the migration of facial branchiomotor neurons in developing zebrafish embryos". Carolina Fiallos Oliveros and Toshio Ohshima. The International Journal of Developmental Biology. *in press.*

"Quantification of native mRNA dynamics in living neurons using fluorescence correlation spectroscopy and reduction-triggered fluorescent probes". Hirotaka Fujita, Ryota Oikawa, Mayu Hayakawa, Fumiaki Tomoike, Yasuaki Kimura, Hiroyuki Okuno, Yoshiki Hatashita, Carolina Fiallos Oliveros, Haruhiko Bito, Toshio Ohshima, Satoshi Tsuneda, Hiroshi Abe, and Takafumi Inoue. JBC. *in press.*

Poster presentation

Carolina Fiallos Oliveros and Toshio Ohshima "CRMP2 is required for the migration of facial branchiomotor neurons in developing zebrafish embryos". The 25th Japanese medaka and zebrafish meeting. Sept 4th, 2019